SEMMELWEIS EGYETEM

DOKTORI ISKOLA

Ph.D. értekezések

2732.

KISS ANNA RÉKA

Szív-és érrendszeri betegségek élettana és klinikuma
című program

Programvezető: Dr. Merkely Béla, egyetemi tanár

Témavezetők: Dr. Merkely Béla, egyetemi tanár

Dr. Szűcs Andrea, egyetemi adjunktus

Left ventricular noncompaction:
From hypertrabeculation to heart failure

Ph.D. Thesis

Anna Réka Kiss MD

Doctoral School of Basic and Translational Medicine

Semmelweis University

Supervisors: Andrea Szűcs MD, Ph.D

Béla Merkely MD, D.Sc

Official reviewers: Réka Faludi MD, Ph.D

Zoltán Pozsonyi MD, Ph.D

Head of the Complex Examination Committee:

István Karádi MD, D.Sc

Members of the Complex Examination Committee:

Péter Andréka MD, Ph.D.

Henriette Farkas MD, Ph.D.

Budapest

2022

Table of Contents

List of Abbreviations

bSSFP: balanced steady-state free precession

CMR: cardiac magnetic resonance

DCM: dilated cardiomyopathy

EDV: end-diastolic volume

EDVi: end-diastolic volume index

EF: ejection fraction

ESV: end-systolic volume

ESVi: end-systolic volume index

FT: feature-tracking

GA: gadobutrol

GCS: global circumferential strain

GD: gadobenate dimenglumine

GLS: global longitudinal strain

GRS: global radial strain

ICC: intraclass correlation coefficient

LGE: late gadolinium enhancement

LV: left ventricle

LVNC: left ventricular noncompaction

MRI: magnetic resonance imaging

post-CA: post-contrast agent

post-GA: postgadobutrol

post-GD: post- gadobenate dimenglumine

pre-CA: pre-contrast agent

pre-GA: pregadobutrol

pre-GD: pregadobenate dimenglumine

PTMi: end-diastolic papillary and trabeculated myocardial mass index

RBR: rigid body rotation

ROT: rotation

SA: short axis

SD-TTP-CS: standard deviation of time-to-peak circumferential strain

SD-TTP-LS: standard deviation of time-to-peak longitudinal strain

SV: stroke volume

SVi: stroke volume index

TMi: end-diastolic total myocardial mass index

1. Introduction

1.1. Cardiac trabeculation

Myocardial trabeculae appear at the end of the fourth week of gestation in humans (1). During the early phase of trabecular development, a thick trabecular meshwork is formed mediated by cardiomyocyte differentiation and terminal proliferation and maintained by ligand-receptor interactions between endocardial-endocardial and endocardial-myocardial cells (1, 2). By the end of the eighth week of gestation in humans, ventricular septation is complete, and a significant increase in the proportion and thickness of the compact myocardium is seen. At the same time, the remaining trabeculation becomes rearranged and produces a definitive pattern specific to the ventricles (1). Although several growth factors and intracellular signaling pathways have been identified in trabecular development, the compaction process of trabeculated myocardium into a compact layer still lacks compelling evidence (2, 3).

The role of ventricular trabeculation during cardiac development in the embryonic phase is to facilitate nutrient and gas exchange in the heart muscle before developing coronary arteries (1). However, its role in the developed heart is not fully understood. Observational studies suggest that trabeculation is part of a mechanism for efficient filling and emptying of the chambers (4). It has been hypothesized that trabeculation provides mechanical leverage during early systolic ejection through contraction (1). Paun et al. developed a geometrical model to analyze the performance of the trabeculated left ventricle (LV) in the presence and absence of trabeculae. They suggested that the trabeculated ventricle requires less strain to perform the ejection, and trabeculation allows the production of a higher stroke volume (SV) with the same strain (4). Accordingly, less trabeculation causes unnecessarily large strains in the ventricle, which can be reduced with more trabeculation **(Figure 1)**.

By and large, there is a search for an optimum in cardiac development: ventricular hypertrabeculation commonly leads to early embryonic lethality in small animal models, indicating that a significant reduction in trabeculation prevents the developing heart from functioning as an effective organ (2). However, excessive trabeculation hampers the development of the necessary strain and reduces the space occupied by blood, leading to ventricular dilatation and even cardiac dysfunction in some cases (4).

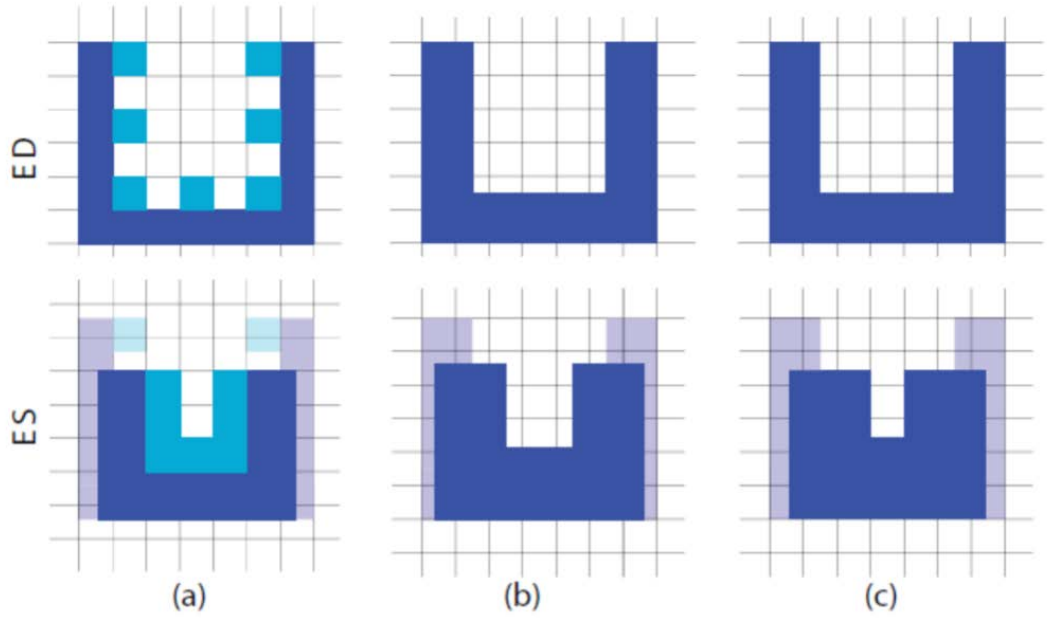

Figure 1. The impact of trabeculation on stroke volume and strain by Paun et al. Panel (a) show the ventricle in its initial configuration with trabeculations (trabeculation - light blue, compacted myocardium – dark blue) and the change in area during contraction (change in areas in 16 squares); panel (b) shows the contraction of the cavity that has only a compacted myocardium (change in areas in 13 squares); panel (c) shows the contraction of the cavity that only has a compacted myocardium and maintains the change in area (18 squares) (4).
ED: end-diastole, ES: end-systole

1.1.1. Ventricular trabeculation in physiological conditions

The amount of LV trabeculation in healthy adults has been studied with cardiac magnetic resonance (CMR); however, generally accepted normal reference ranges are not in use due to the lack of consensus on the measurement technique (5-10). A more accessible approach was introduced to differentiate between normal and excessive LV trabeculation: the ratio of the thickness of trabeculated (noncompacted) and compacted myocardial layers measured in long- or short-axis echocardiographic/CMR images (11, 12).

A broad spectrum of ventricular trabeculation exists across *healthy populations* (13-16). According to large, population-based, multiethnic studies, such as MESA and TASCFORCE, excessive LV trabeculation is present in 15-43% of patients and is influenced by ethnicity and sex **(Figure 2)** (13-15). African American and Hispanic racial backgrounds are associated with increased trabeculation compared with white backgrounds, while Chinese Americans have a tendency for reduced LV trabeculation (14). Additionally, the thickness of trabeculae and trabecular complexity are positively associated with the male sex (13, 14). Individuals with

more LV trabeculation tend to have higher LV end-diastolic (EDV) and end-systolic volumes (ESV) and a lower ejection fraction (EF); however, according to the results of a 9.5-year follow-up study, excessive LV trabeculation was not associated with a further increase in LV volumes or a decrease in ventricular function (13, 15, 16). Hence, a greater extent of ventricular trabeculation is benign and does not seem to have clinical implications in healthy individuals (16).

Other physiological conditions, such as *vigorous physical activity* and *pregnancy*, can be associated with acquired and reversible LV hypertrabeculation **(Figure 2)** (17, 18). Gati et al. described that 8.1% of the 1146 studied athletes had excessive LV trabeculation, and further studies confirmed the association between vigorous physical activity and increased ventricular trabeculation and the reversible nature of this hypertrabeculation (17, 19, 20). A study including 102 primigravida pregnant women demonstrated that de novo LV trabeculation occurred in 25% of the studied individuals, which showed complete resolution in 69% of the postpartum period (18). An additional 12% showed gradual regression over the 2-year follow-up period (18). It was suggested that the development of more trabeculation is an adaptive mechanism of the heart used to increase cardiac output and increase preload, which is present in both high-intensity physical activity and pregnancy (4, 18). This cardiac remodeling allows the ventricle to produce an increased stroke volume if required or keep the SV at the required level with a lower strain in case of increased preload (4).

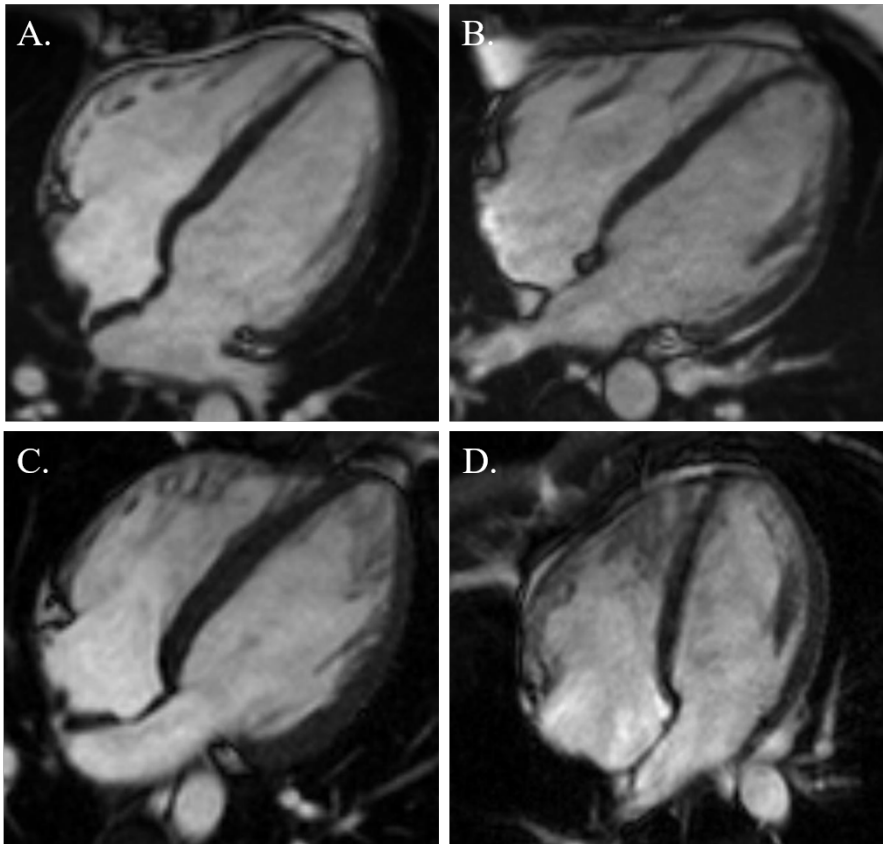

Figure 2. Four-chamber long-axis CMR images of a healthy volunteer with a normal amount of LV trabeculation (A), a healthy volunteer (B), an elite athlete (C), and a healthy black participant (D) whom all presented with excessive LV trabeculation.

1.1.2. Ventricular trabeculation in pathologic conditions

Excessive ventricular trabeculation is the principal anatomic characteristic of *left ventricular noncompaction (LVNC),* in which prominent abnormal trabeculae are present in the apical part of the LV and form a noncompacted myocardial layer that is thicker than the compacted myocardium **(Figure 3)** (2). It is a rare condition that can be diagnosed in infants (0.81 per 100,000 infants), children (0.12 cases per 100,000 children) and adults (prevalence: 0.014%) (21). Several morphologic criteria have been presented for both echocardiography and CMR, as later discussed in Section 1.3 (22). Clinical manifestations range from no symptoms to heart failure, arrhythmias, and thromboembolic events (23). However, to differentiate between physiologic LV hypertrabeculation and LVNC, an integrated diagnosis should be made, and both morphologic criteria and the patient's clinical history should be considered (24). Suppose only morphologic criteria are fulfilled, but the patient's clinical history, family history, ECG, and Holter monitoring are negative and late gadolinium enhancement (LGE) is not present. In that case, it is considered a noncompaction phenotype, and no follow-up is necessary (24).

LVNC can be diagnosed if at least one clinical sign (symptoms, positive family history, the presence of arrhythmias on ECG or Holter, the presence of late gadolinium enhancement, heart failure, positive genetic test result) is present in addition to the specific morphologic features (24). The prognosis of LVNC without clinical manifestations is good, although life expectancy can be reduced in the presence of heart failure, malignant arrhythmias, and thromboembolic events (25, 26). In the latter case, the risk of death from cardiovascular causes is similar to that in patients with dilated cardiomyopathy (DCM) (26).

LVNC can be inherited or sporadic. The genetic background of inherited LVNC is heavily researched, but most of the associated mutations are in the same genes that cause other types of cardiomyopathies as well (21). Thus, LV hypertrabeculation/noncompaction can be observed in cardiomyopathies with overlapping phenotypes in *dilated*, *hypertrophic (HCM)*, and *arrhythmogenic cardiomyopathy* **(Figure 3)** (27).

LV hypertrabeculation/noncompaction can be associated with *congenital heart diseases* (e.g., patent ductus arteriosus, atrial/ventricular septal defects, Ebstein anomaly or hypoplastic left heart syndrome) due to genetic mutations or hemodynamic factors (27, 28).

An increased preload, increased afterload, and chronic anemia might trigger myocardial remodeling, resulting in acquired LV hypertrabeculation, which has been described in patients with *β-thalassemia*, *chronic kidney disease*, and *sickle cell anemia* (29-31).

A different approach was proposed by Arbustini et al., who concluded that LVNC could be regarded as an isolated entity or a trait that can recur in various cardiac and noncardiac diseases (27). According to this assumption, LVNC can be grouped as follows: (1) isolated LVNC with normal LV function; (2) LVNC with LV dilation and dysfunction at onset; (3) LVNC in the presence of DCM, HCM, or arrhythmogenic cardiomyopathy; (4) LVNC associated with congenital heart diseases; (5) syndromes with LVNC; (6) acquired and potentially reversible isolated LVNC; and (7) right ventricular noncompaction (27).

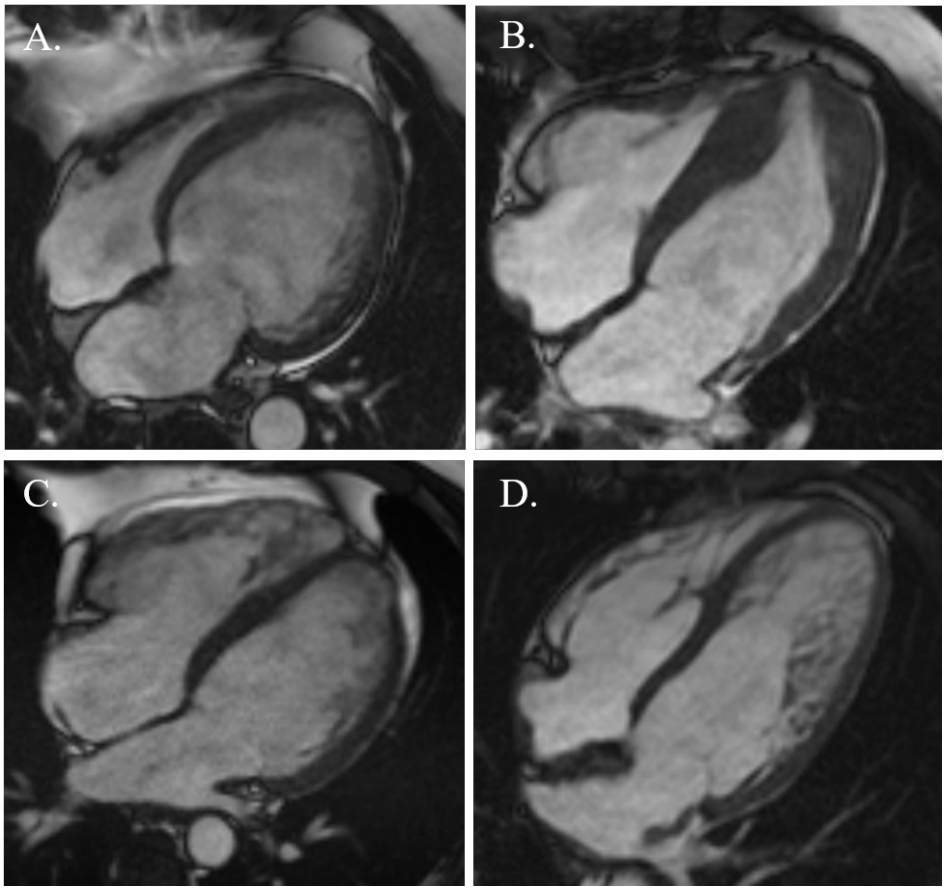

Figure 3. CMR images of patients with dilated cardiomyopathy (A), hypertrophic cardiomyopathy (B), arrhythmogenic cardiomyopathy (C), and left ventricular noncompaction (D).

1.2. Cardiac magnetic resonance

The first recognizable magnetic resonance images of the human heart were obtained in 1981. However, the significant problem of motion artifacts came from breathing and was not solved until 1991, when the method of ECG gated segmented data acquisitions for cine imaging was introduced. The current cine balanced steady-state free precession (bSSFP) pulse sequence was introduced in 1999 (32).

Since then, due to its accuracy and prognostic value, CMR has become the gold standard noninvasive imaging tool in visualizing and assessing cardiac anatomy, volumes and function, and myocardial tissue characterization (33). Cine imaging covering the ventricles from base to apex is used for measuring volumes and function, while regional wall motion abnormalities can also be assessed using multiple planes (34). Wall thickness can be accurately measured in hypertrophic states, and CMR affords superior visualization of the apical structures (aneurysms, apical HCM, LVNC) (35).

Noninvasive tissue characterization can be achieved with T1 and T2 imaging. Gadolinium-based contrast agents are paramagnetic, T1-shortening agents distributed within intravascular and extracellular compartments (35). Myocardial fibrosis causes the expansion of the extracellular space, leading to a higher concentration of gadolinium-based contrast agents and a hyperenhanced signal in this area (late gadolinium enhancement) (36). The pattern of LGE is characteristic of different diseases and plays a significant role in the diagnosis, e.g., subendocardial, and transmural LGE is typical of ischemic etiology; midwall LGE can be present in dilated cardiomyopathy or myocarditis, and subepicardial LGE might be present in myocarditis or sarcoidosis **(Figure 4)** (34).

Further, CMR tissue characterization techniques include T1 and T2 mapping and extracellular volume quantification (36). Last but not least, 4D-Flow provides quantitative information on flowmetry across the valves or within the chambers (37).

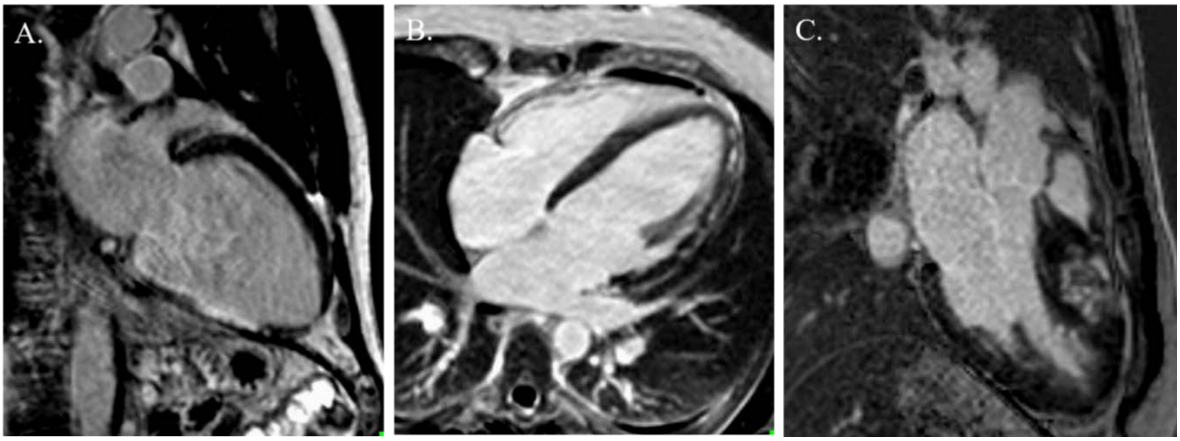

Figure 4. Late gadolinium enhancement in myocardial infarction (A), myocarditis (B), and hypertrophic cardiomyopathy (C).

1.2.1. The role of cardiac magnetic resonance in the assessment of left ventricular noncompaction

Transthoracic echocardiography has been used for diagnosing LVNC since the first morphologic criteria were described in 1990 by Chin et al. (38). Since then, several criteria have been established, and echocardiography is still the imaging method of choice to identify LV hypertrabeculation and follow-up patients (24, 38). However, the diagnosis might be incorrect when echocardiography is used as the sole imaging modality (39). Further evaluation with CMR is recommended to confirm the diagnosis, as it provides a better morphologic characterization of the myocardium due to the high spatial resolution.

Several groups have worked on developing CMR diagnostic criteria for LVNC; however, there is a lack of consensus on which criteria should be used routinely (40). Petersen et al. were the

first to participate in this evaluation. They measured the end-diastolic thickness of noncompacted and compacted myocardial layers in the long-axis view and found that the ratio of these layers with a cutoff of 2.3 has high diagnostic accuracy in identifying LVNC from other conditions presenting with LV hypertrabeculation **(Figure 5)** (11).

Another diagnostic approach is the measurement of noncompacted myocardial mass: a trabeculated mass >20% of the global LV mass has been found to have a sensitivity and specificity of 93.7% to differentiate pathologic trabeculation **(Figure 5)** (41). Interestingly, Grothoff et al. also measured the percentage of noncompacted myocardial mass, but they found that the optimal cutoff was 25%, slightly different from the previous cutoff (42). They also described a trabeculated myocardial mass >15 g/m^2 as highly sensitive and specific to LVNC (42). Although we need to mention that these criteria do not consider sex, however, men have a higher LV trabeculated myocardial mass due to hormonal and biometric causes (10).

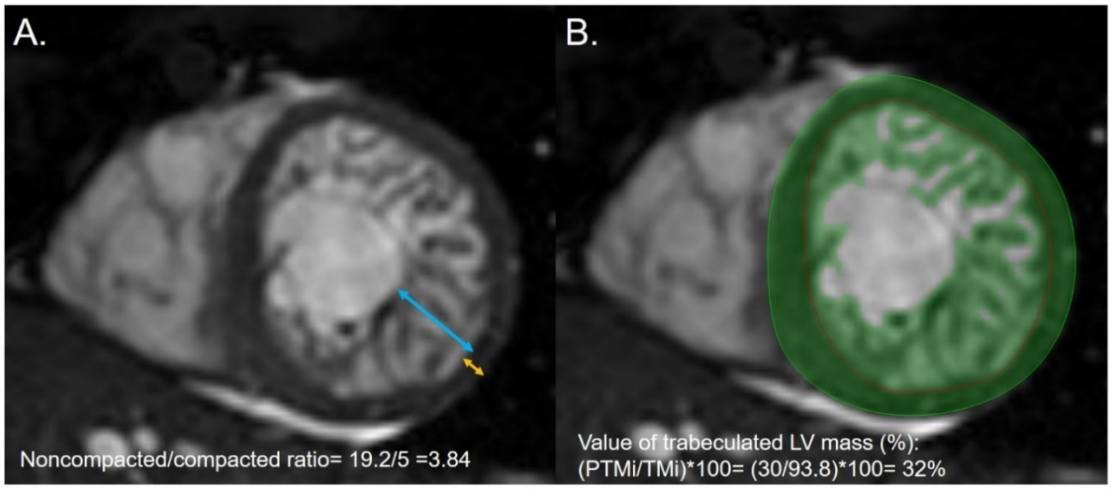

Figure 5. Short-axis image of a participant who fulfilled Petersen's (A) and Jacquier's (B) morphologic criteria of left ventricular noncompaction. The orange line represents the compacted myocardial layer, the blue line represents the noncompacted layer (A), the green area represents the compacted and noncompacted myocardium, and the red line borders endocardial trabeculation (B).

LV: left ventricle, TMi: left ventricular total myocardial mass, PTMi: left ventricular papillary and trabeculated muscle mass

Endocardial trabeculation creates a highly irregular endocardial border, and its complexity can be measured using fractal analysis (43). This method quantifies complex geometric patterns. The fractal dimension is a unitless measure index that shows how completely the complex structure fills its space. The higher the fractal dimension, the more complex the structure. Captur et al. described patients with LVNC as having significantly higher fractal dimensions

than healthy controls (43). They also proposed a cutoff for the fractal dimension as a diagnostic marker of LVNC (43). However, this technique requires specific software and reference ranges for healthy individuals, which have not been established.

In the following years, it became evident that the sole use of morphologic criteria results in overdiagnosis, as it is fulfilled in up to 43% of the healthy population (13). For this reason, a more complex approach was recently proposed that combines morphologic criteria with the patient's clinical history to establish the diagnosis (24).

As already mentioned, tissue characterization is a great advantage of CMR. A meta-analysis including four studies assessed the predictive value of LGE in LVNC (44). They concluded that the presence of LGE was a predictor of major adverse cardiovascular events and was associated with a worse prognosis in patients with LVNC independent of LV function (44).

Novel technologies, such as deformation analysis might provide additional information for diagnosis and prognosis. A large number of speckle-tracking echocardiography studies were conducted to describe the myocardial deformation pattern of patients with LVNC and to develop new and additional diagnostic criteria (45-47). Nonetheless, the results are controversial, and comprehensive information is not available about the feature-tracking strain characteristics of LVNC patients with different levels of LV EF deterioration.

1.2.2. Threshold-based trabecular and papillary muscle mass quantification

According to the position statements for standardized image interpretation and postprocessing in CMR, trabeculated and papillary muscles should be included with the myocardium as part of the LV mass if possible (33). Inclusion in the blood volume is also acceptable and is widely used, as not all evaluation tools allow for the inclusion of trabeculated and papillary muscle to LV myocardium without manual drawing of contours. Manual exclusion of the trabeculation by drawing nonconvex endocardial contours has demonstrated high intra- and interobserver variability (33, 48). Several studies have indicated that including trabeculated and papillary muscles in the blood pool significantly changes the measured volumetric, functional, and myocardial mass values (49, 50). Yet, these values correlate well with each other (49, 50). Accordingly, the applied normal values should be selected. Quantification of the trabeculated myocardium is not part of the routine assessment, but it can be relevant in patients with LV hypertrophy or hypertrabeculation (42, 51).

In the past ten years, different vendors have developed slightly different algorithms to quantify trabeculation. However, they are all based on high-resolution imaging of the LV with great visual contrast between the darker myocardium and the bright blood pool using cine bSSFP

sequences (52-54). Hautvast et al. proposed a fuzzy thresholding algorithm where thresholds are determined based on image characteristics and are examination specific (6, 52).

Jaspers et al. proposed a semiautomatic threshold-based method where the epicardial contour served as the initialization **(Figure 6)** (53). Within the epicardial contour, the algorithm estimated the signal intensity of blood and myocardium and calculated a blood percentage value for any given voxel using an equation described by them (53). Thus, voxels were classified as either blood or muscle based on their signal intensity. Based on visual inspection, the signal intensity threshold can be manually adjusted between 1 and 100% separately for end-systolic and end-diastolic phases. This method has been validated against aortic flow measurements and provides a more accurate evaluation of LV volumes and mass than conventional contour-based techniques (55). It is highly reproducible, and the evaluator's experience did not have any considerable effect on the measured parameters (50).

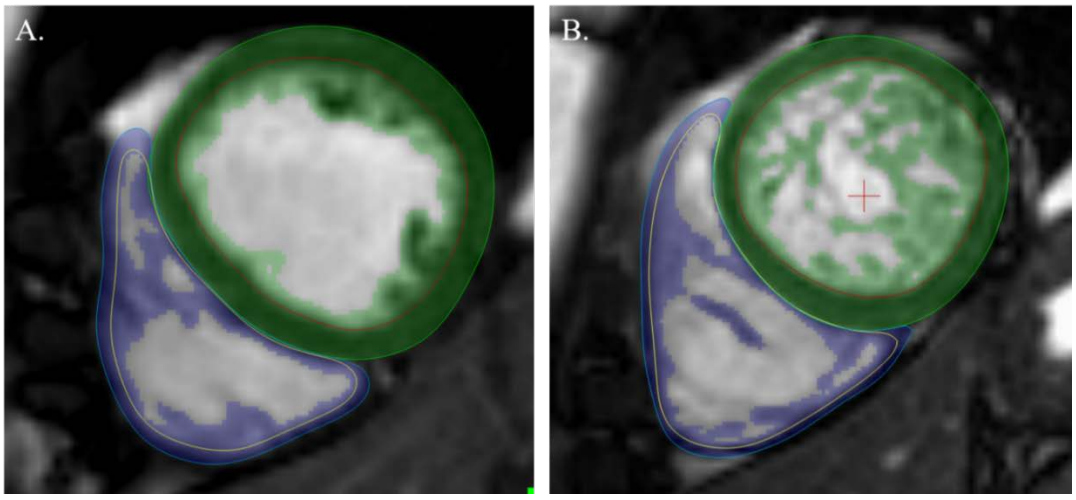

Figure 6. Representative image analysis with threshold-based papillary and trabeculated muscle quantification software and the calculated left ventricular parameters of healthy participants (A) and a patient with left ventricular noncompaction (B). The green and blue areas represent the myocardial mass, including the left and right ventricles' endocardial trabeculation (included in the endocardial contours). The threshold was set to 50%.

A few limitations regarding these threshold-based software programs should be mentioned. The current ejection fraction and volume quantification uses a stack of thick short-axis slices, and 8-10 mm are standard for Z-direction spatial resolution. Moreover, trabeculae and papillary muscles do not cross the slice in an exactly perpendicular fashion, which creates partial volume effects. Depending on the actual path of the trabeculae, this feature will influence the threshold-based quantification (53, 56).

1.2.3. Feature-tracking deformation analysis

Assessment of LV function remains challenging. EF is the most commonly used parameter for this process; however, its reproducibility is suboptimal because it does not reflect regional LV function (57). Further limitations also arise from its volumetric nature (57). The need for more accurate characterization of LV mechanics has emerged, and the use of strain for the noninvasive evaluation of myocardial deformation has spread.

Myocardial strain measures the degree of deformation of a myocardial segment from its initial length (in end-diastole, L_0) to its maximum length (in end-systole, L_1): strain = $(L_1-L_0)/L_0$ (58). The different spatial components of myocardial contraction can be studied using longitudinal, radial, or circumferential strain. *Longitudinal strain* represents longitudinal shortening from base to apex (negative value); *radial strain* indicates LV thickening and thinning during the cardiac cycle toward the center of the LV cavity (positive value); and *circumferential strain* derives from LV myocardial shortening along the circular perimeter measured on a short-axis view (negative value) (58). These strain values can describe both *global* and *segmental* LV deformation.

The ability to detect early myocardial dysfunction and the prognostic role of strain measurement have been shown in several cardiovascular diseases, resulting in its use as part of routine examinations (58).

Tissue tagging was the first method that allowed deformation analysis with CMR (59). CMR tagging magnetically labels different regions of the myocardium with selective radiofrequency saturation planes and pulses. Tag lines will move along with the myocardium during contraction; thus, tracking these tags allows direct evaluation of myocardial strain (57). Tagging has been validated extensively using both in vitro and in vivo models and is considered the reference standard modality for CMR strain quantification (57). Although it has several limitations, such as low temporal resolution, it potentially underestimates strain at higher heart rates and requires dedicated acquisition sequences and special postprocessing software (57).

In contrast, feature-tracking (FT) technology is a postprocessing method that gained popularity by allowing measurements without additional sequences. It is an optical flow 2D method that can be applied to routinely acquired cine bSSFP sequences. It is based on identifying features in the image and tracking them in subsequent frames throughout the cardiac cycle **(Figure 7)** (58). The tracked features are anatomic elements on the myocardial cavity tissue boundary and are found by the maximum-likelihood method between two regions of interest between two frames (58). Manual contour detection of the endocardium, epicardium, and mitral valve

annular plane is needed for automatic border tracking of the software (58). Longitudinal strains are estimated from long-axis SSFP cine images, while short-axis cine images are used for circumferential and radial strain measurements. Although FT was developed for 2D images, it can also be applied for 3D image tracking. There are a few limitations. This method lacks a relevant validation process, and thus, its clinical application is questionable. Additionally, the reproducibility of segmental strain is worse than the gold-standard tissue tagging, and there is high variability in normal strain values between different vendors; thus, there is a lack of an accepted normal reference range (57, 60).

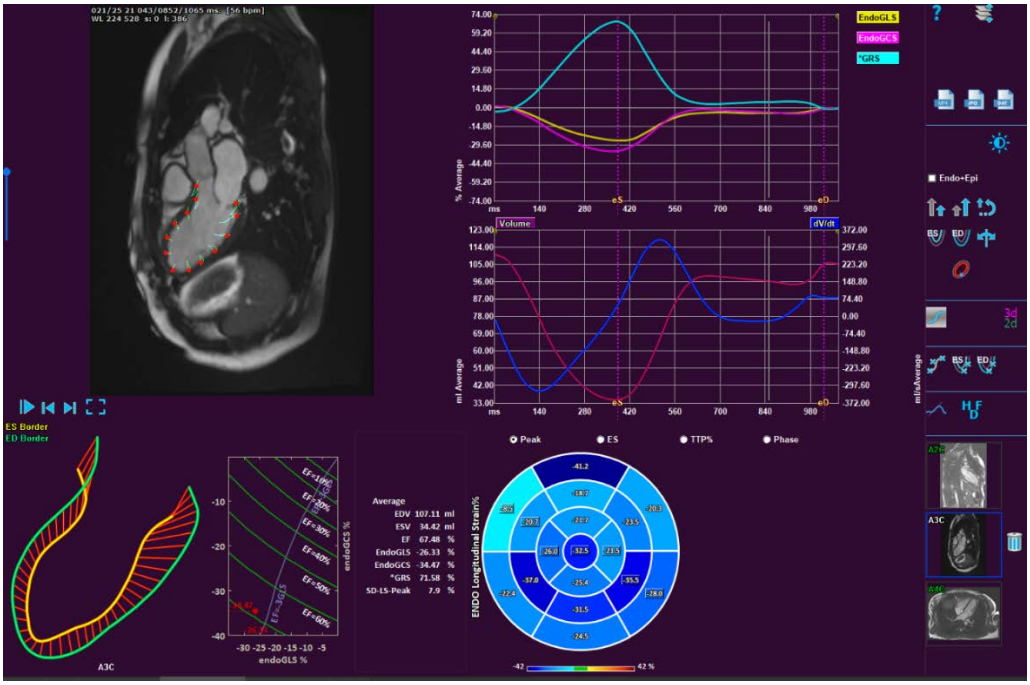

Figure 7. Representative image analysis with the feature-tracking software.

1.3. Questions and controversies about left ventricular noncompaction

Nevertheless, LVNC is a widely studied entity with more than 2000 publications in the field, and our understanding of ventricular trabeculation and LVNC remains in its infancy compared with other cardiomyopathies.

First, LVNC was defined as a genetic cardiomyopathy by the American Heart Association; however, many scientists describe LVNC as a trait shared by many pathologic conditions and not a single disease (61). Developments in imaging technology have improved the visualization of ventricular trabeculation, although a standardized protocol is not available for its quantification. Questions including the type of postprocessing measurement and whether the use of contrast agent has an effect on trabecula quantification have been raised.

Developments in the field of imaging have also resulted in an overdiagnosis of LVNC (61). However, it is still not clear whether all subjects with LVNC have cardiomyopathy or if LVNC describes a phenotype with a spectrum of normal variants, physiologic-to-pathologic remodeling and cardiomyopathy (62). Labeling healthy individuals with LVNC has a negative impact on the subject and on health care resources (62). The sole use of morphologic criteria does not identify patients with true cardiomyopathy. The addition of a detailed clinical history and family anamnesis to the diagnosis helps to discover patients who should undergo genetic testing, which can then reveal the presence of genetic causes of cardiomyopathy (62). However, genetic testing is not widely available. Morphologic criteria do not predict outcome, but novel imaging modalities, such as deformation analysis, might help differentiate between a normal anatomic phenotype and LVNC cardiomyopathy (62). Speckle-tracking echocardiography studies have already been published about the myocardial deformation pattern of patients with LVNC and the development of new and additional diagnostic criteria; however, the results are controversial (45-47). Furthermore, CMR FT studies are not available.

2. Objectives

The goal of our research was to create an optimal CMR study protocol for patients with ventricular hypertrabeculation and to describe the left ventricular volumetric, functional and deformation characteristics of patients with LVNC with good to severely reduced ventricular function.

2.1. The effect of contrast agents on left ventricular parameters calculated by a threshold-based software module

To shorten the scan time, bSSFP short-axis cine images are often acquired after contrast agent administration, which is a global practice and a recommended technique for CMR examinations. This study was designed to confirm our experience with the postprocessing evaluation of scans made after the injection of gadolinium-based contrast material, namely, that endocardial trabeculation is more difficult to detect. We aimed to quantify the effect of contrast agent on calculated parameters of patients with LVNC and healthy participants using threshold-based papillary and trabeculated muscle quantification postprocessing software. Furthermore, we studied the effects of different types of gadolinium-based contrast agents on the applicability of threshold-based papillary and trabeculated muscle quantification software.

2.2. Left ventricular characteristics of noncompaction phenotype patients with good ejection fraction

We aimed to describe the LV volumetric parameters and the myocardial and trabeculated muscle mass of a large cohort who fulfilled the morphological criteria of LVNC and had good LV function and no comorbidities and to study the LV strain characteristics with FT. Male and female patients were compared to describe the differences between sexes. Moreover, we investigated the different cutoff points of LV trabeculated muscle mass for male and female LVNC patients to differentiate them from healthy subjects.

2.3. Left ventricular characteristics of patients with left ventricular noncompaction at different deterioration levels of ventricular function

As we did not find comprehensive information about the feature-tracking strain characteristics of LVNC patients with different levels of LV EF deterioration, our aim was to describe the changes in LV global and regional strain parameters that occur in patients with noncompacted LV with good to significantly reduced LV ejection fraction and to compare their characteristics with those observed in healthy controls. Furthermore, we assessed disease-specific strain characteristics.

3. Methods

3.1. Study design and study population

3.1.1. Study design and study population to examine the effect of contrast agent on left ventricular parameters calculated by a threshold-based software module

This study was conducted in 2016-2017 at the Semmelweis University Heart and Vascular Center. Twenty patients who fulfilled the CMR morphologic criteria of LVNC set by Petersen et al. (noncompacted/compacted ratio > 2.3, **Figure 5**) and Jacquier et al. (trabeculated LV mass >20% of the total LV mass, **Figure 5**) with a good LV ejection fraction and without any additional cardiac abnormalities or cardiovascular diseases were prospectively enrolled (11, 63). The exclusion criteria were the presence of congenital heart disease, ischemic heart disease, other cardiomyopathies or myocarditis in the patient's history. Nineteen healthy volunteers without any known cardiovascular or other systemic diseases were enrolled for the control group. The baseline parameters of the LVNC patients and healthy individuals are reported in **Table 1**. Ethical approval was obtained from the Semmelweis University Regional and Institutional Committee of Science and Research Ethics, and all participants provided informed consent (166/2017).

The CMR study protocol was as follows: after the short axis cine images were acquired, either gadobutrol ((GA), Gadovist, Bayer-Schering, 0.16 ml/kg) or gadobenate dimenglumine ((GD), MultiHance, Bracco, 0.25 ml/kg) was injected intravenously (**Figure 8**). Each included individual received only one type of contrast agent, which was decided randomly. GA was administered to 12 LVNC patients and 12 healthy normal participants, and GD was administered to 8 LVNC patients and 7 healthy participants **(Table 1)**. After the contrast material was injected, another set of SA cine images was started after two minutes in the same location.

Figure 8. Study protocol of the effect of contrast agent on left ventricular parameters calculated by a threshold-based software module project.

Pre-CA: precontrast agent, post-CA: postcontrast agent, SA: short axis

Table 1. Baseline characteristics of the left ventricular noncompaction and healthy study groups.

EDV: end-diastolic volume, EF: ejection fraction, ESV: end-systolic volume, LVNC: left ventricular noncompaction, TMi: left ventricular total myocardial mass, PTMi: left ventricular papillary and trabeculated muscle mass

	LVNC n=20	Healthy n=19	p
Gadobutrol (n)	12	12	-
Gadobenate dimenglumine (n)	8	7	-
Age (years)	41.7±16.3	37.9±16.6	0.474
LV-EF (%)	66.1±5.2	67.8±5.5	0.975
LV-EDVi (ml/m²)	74.0±13.6	69.7±11.9	0.301
LV-ESVi (ml/m²)	25.3±7.3	22.6±5.7	0.196
LV-TMi (g/m²)	82.5±17.5	71.3±13.6	**0.032**
LV-PTMi (g/m²)	25.0±6.6	19.4±2.6	**0.002**

3.1.2. Study design and study population to examine the left ventricular characteristics of noncompaction phenotype patients with good ejection fraction

Eighty-one patients were included in this retrospective study conducted at the Semmelweis University Heart and Vascular Center. All of them fulfilled the morphologic criteria of LVNC set by Petersen et al. (noncompacted/compacted ratio > 2.3, **Figure 5**) and Jacquier et al. (trabeculated LV mass >20% of the total LV mass, **Figure 5**), had good LV ejection fraction (>55%), and no known cardiovascular or other comorbidities (age: 35.6±14.7 years, male: n=44) (11, 63). The exclusion criteria were a reduced LV ejection fraction (<55%), the presence of ischemic, valvular or congenital heart disease, the presence of significant comorbidities (e.g., diabetes, hypertension, chronic kidney disease, chronic liver failure), and technical reasons (artifacts, short-axis cine images performed after the injection of contrast agent) (64, 65). We selected 81 sex-matched healthy volunteers from similar age groups for the patient group who did not have any cardiovascular or other systemic diseases and who did not have excessive endocardial trabeculation according to the abovementioned criteria (age: 38.2±12.8 years, male: n=44). Baseline characteristics are shown in **Table 2**. Ethical approval was obtained from the Semmelweis University Regional and Institutional Committee of Science and Research Ethics, and all participants provided informed consent (165/2017).

Table 2. Baseline characteristics of the included left ventricular noncompaction and healthy study groups.

EF: ejection fraction, LVNC: left ventricular noncompaction

	LVNC	Control	p
Number of participants (n)	81	81	-
Male/Female (n)	44/37	44/37	-
Age (years)	35.6±14.7	38.2±12.8	0.228
Male age (years)	34.3±14.6	38.4±10.4	0.131
Female age (years)	37.1±14.8	37.9±15.2	0.817
EF (%)	65.9±5.2	70.2±5.0	**<0.001**

3.1.3. Study design and study population to examine the left ventricular characteristics of patients with left ventricular noncompaction at different deterioration levels of ventricular function

This retrospective study was conducted at the Semmelweis University Heart and Vascular Center. Thirty-one LVNC patients with good LV function (Group A, EF> 50%, age: 49.5±10.9 years, male: n=21) and 31 LVNC patients with a reduced LV ejection fraction (Group B, EF< 50%, age: 54.4±12.1 years, male: n=21) were included according to the following criteria: (1) fulfillment of the CMR criteria of LVNC set by Petersen et al. and Jaqcuier et al., (2) no concomitant ischemic or congenital heart disease and no presence of other cardiomyopathies, (3) no significant comorbidities, and (4) acquisition of CMR short- and long-axis cine images before injection of the contrast agent with no artifacts (11, 63, 66). In addition to this patient population, we included 31 age- and sex-matched healthy control subjects (age: 48.8±9.6 years, male: n=21) who did not have any cardiovascular or other systemic diseases and did not have excessive endocardial trabeculation in the apical part of the LV according to the applied criteria. We divided Group B by LV ejection fraction into two subgroups: Group B-1 contained LVNC patients with an LV ejection fraction between 35 and 50% (n=13, age: 51.5±13.0 years, male: n=8), and Group B-2 contained patients with an LV ejection fraction lower than 35% (n=18, age: 56.6±11.3 years, male: n=13). Ethical approval was obtained from the Central Ethics Committee of Hungary, and all participants provided informed consent (OGYÉI/7397/2019). **Table 6** shows the baseline characteristics of the studied groups.

3.2. Image acquisition and analysis

CMR examinations were performed on a 1.5 T MRI machine (Achieva, Philips Medical System, Eindhoven, the Netherlands and Magnetom Aera, Siemens Healthineers, Erlangen, Germany) and a 5-channel cardiac coil. Retrospectively gated, balanced, steady-state free precession cine images in 2-, 3-, and 4-chamber long-axis views and breath-hold short-axis cine images were acquired from base to apex with full coverage of the left and right ventricles. The temporal resolution was twenty-five phases per cardiac cycle. The slice thickness was 8 mm with no interslice gap; the field of view was 350 mm on average, adapted to body size. Cine images were performed before injection of the contrast agent (gadobutrol, 0.15 ml/kg), when it was given, except in "the effect of contrast agent on left ventricular parameters calculated by a threshold-based software module" project (detailed protocol in Section 3.1.1).

Medis Suite version 3.0 was used for the postprocessing analysis (Medis Medical Imaging Systems, Leiden, the Netherlands). Semiautomatic tracing with manual correction of the endo- and epicardial contours of the left and right ventricles was performed on the short-axis cine images by two observers as described by others (53). The interobserver agreement values are presented in the Section 4. LV volumetric and functional and myocardial mass values were calculated with the threshold-based papillary and trabeculated muscle quantification module of the software (MassK). The threshold was set to 50%, and manual correction was not applied

The QStrain module of the Medis Suite software was used for the feature-tracking strain analysis (Medis Suite, version 3.0, Medis Medical Imaging Systems, Leiden, the Netherlands). To determine the subendocardial strain, endocardial contours were drawn in end-diastole and end-systole in the 2-, 3-, and 4-chamber long-axis and short-axis views of the LV, including endocardial trabeculation, as described by others (67).

3.3. Studied parameters

3.3.1. Studied parameters of the effect of contrast agent on left ventricular parameters using a threshold-based software module project

Both the first (before contrast agent administration (pre-CA)) and the second (after contrast agent administration (post-CA)) short axis scans were analyzed.

The following LV parameters were calculated and converted to body surface area using the Mosteller formula: ESV, EDV, EF, end-diastolic total myocardial mass (TM), and end-diastolic papillary and trabeculated myocardial mass (PTM) (68). The normal LV dimensions provided by Alfakih et al. were used as reference data which were established without administration of contrast agent (69).

3.3.2. Studied parameters of the left ventricular characteristics of noncompaction phenotype patients with a good ejection fraction

The LV volumetric (ESV, EDV, SV), function (EF), and myocardial mass values (TM, PTM) were measured and indexed to the body surface area using the Mosteller formula (68).
Global longitudinal strain (GLS), global radial strain (GRS), global circumferential strain (GCS), and rotation (ROT) were also assessed. The standard deviation of the time-to-peak strains between segments was analyzed in both the long-axis and short-axis views to determine the degrees of intraventricular synchronous contraction in the longitudinal and circumferential directions (longitudinal mechanical dispersion (SD-TTP-LS) and circumferential mechanical dispersion (SD-TTP-CS)).

3.3.3. Studied parameters of the left ventricular characteristics of patients with left ventricular noncompaction at different deterioration levels of ventricular function

We measured the LV volumetric (EDV, ESV, SV), functional (EF), and myocardial mass values (TM, PTM) and indexed them to the body surface area using the Mosteller formula (68). We further measured the global strain parameters of the LV in the longitudinal, radial, and circumferential directions (GLS, GRS, GCS). To eliminate the possible inaccuracies of the FT segmental strain measurement, we calculated the mean segmental strain values of the apical, mid and basal thirds of the LV in both longitudinal and circumferential directions according to the 17- and 16-segment models (70). To determine the degree of intraventricular synchronous contraction, the standard deviation of the time-to-peak strains between segments was analyzed in the longitudinal and circumferential directions (SD-TTP-LS, SD-TTP-CS). Finally, the systolic peak rotation of the apical and basal parts of the LV was calculated, and the rotation pattern was analyzed. The normal rotation pattern is characterized by a clockwise rotation at the base of the LV (negative value) and a counterclockwise rotation at the apical part of the LV (positive value). By rigid body rotation (RBR), we mean that the apical and basal parts of the LV rotated predominantly in the same direction (47).

3.4. Statistical analysis

3.4.1. Statistical analysis of the effect of contrast agent on left ventricular parameters using a threshold-based software module project

All data are described as the mean and standard deviation. The Shapiro–Wilk test was applied to assess normality. The interobserver agreement was tested with the intraclass correlation coefficient (ICC). A paired-sample t-test was used to assess differences in parameters that had

a normal distribution; otherwise, the Wilcoxon rank sum test was used. P values less than 0.05 were considered significant. MedCalc Statistical Software version 17.9.5 (MedCalc Software, Ostend, Belgium) was used for statistical calculations.

3.4.2. Statistical analysis of the left ventricular characteristics of noncompaction phenotype patients with good ejection fraction

Continuous variables are presented as the mean and standard deviation. The Shapiro–Wilk test was used to assess whether the data fit a normal distribution. The interobserver agreement was tested as presented as the intraclass correlation coefficient (ICC) and a 95% confidence interval. An independent-sample t-test was used to compare parameters that fit a normal distribution; otherwise, a Mann–Whitney test was applied. Receiver operating characteristic curves and optimal cutoff values for the LV trabecular mass index were calculated. P values less than 0.05 were considered significant. MedCalc Statistical Software version 17.9.5 (MedCalc Software, Ostend, Belgium) was used for the statistical calculations.

3.4.3. Statistical analysis of the left ventricular characteristics of patients with left ventricular noncompaction at different deterioration levels of ventricular function

Continuous variables are presented as the mean and standard deviation. Categorical variables are expressed as counts and percentages. The interobserver agreement was tested and presented as the intraclass correlation coefficient (ICC) and a 95% confidence interval. The Shapiro–Wilk test was used to assess normal distributions. Levene's test was used to assess the equality of variances of the tested groups. Differences between the control and LVNC groups were analyzed with one-way analysis of variance and Tukey's post hoc test in cases of a normal distribution and equal variances, while the Welch test and Games-Howell post hoc test were used where variances were unequal. Nonnormally distributed data were analyzed with the Kruskal–Wallis test with Bonferroni correction for multiple comparisons. A p value <0.05 was considered statistically significant. IBM SPSS Statistics (Version 25.0, Armonk, NY) was used for the calculations.

4. Results

4.1. Results of the effect of contrast agent on left ventricular parameters using a threshold-based software module project

Interobserver agreement

The interobserver agreement was tested on ten randomly selected participants. The global ICC, which represents the interobserver agreement of all measured LV parameters, was 0.88 (interpreted as: greater than 0.75 excellent).

Comparison of the pre- and postcontrast agent scans

We compared the parameters calculated from the pre-CA and post-CA scans both in the LVNC and healthy groups and found significant differences in the LV parameters, namely, the EDVi and ESVi were significantly larger, and the LV total and trabeculated myocardial mass were significantly smaller on the post-CA scans in both groups (**Figure 9**).

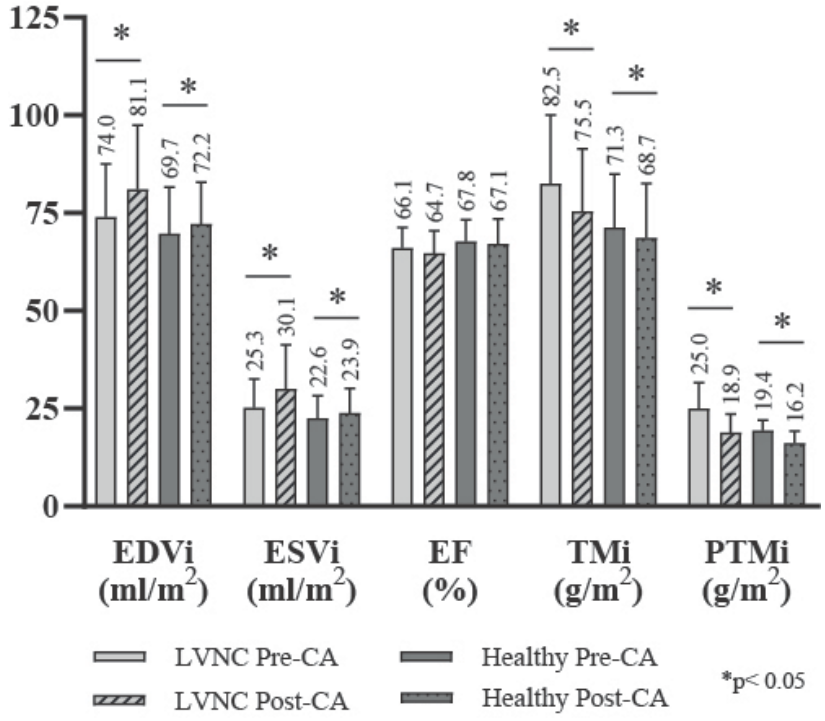

Figure 9. Graphic representation of the calculated parameters of the LVNC and healthy study groups calculated from precontrast and postcontrast scans.

EDVi: end-diastolic volume index, EF: ejection fraction, ESVi: end-systolic volume index, LVNC: left ventricular noncompaction, post-CA: postcontrast agent, pre-CA: precontrast agent, PTMi: end-diastolic papillary and trabeculated myocardial mass index, TMi: end-diastolic total myocardial mass index

Next, the values of the post-CA parameters were subtracted from the values of the pre-CA parameters, and the absolute values were used to compare the differences between the pre- and post-CA parameters of the two groups. The difference between the scans was significantly larger in the LVNC group than in the healthy normal group.

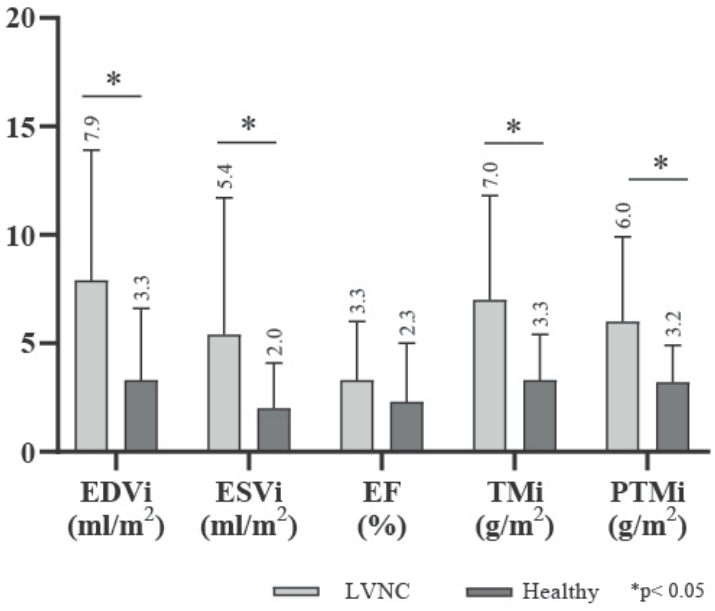

Figure 10. Graphic representation of the comparison of the differences between the pre- and post-CA parameters of the left ventricular noncompaction (LVNC) and healthy groups.

Comparing the effects of different contrast agents

Since different types of contrast agents are in use, we tested whether these agents have similar effects on the studied parameters. We first compared the pre- and post-CA results in the LVNC group (pre-GA vs. post-GA and pre-GD vs. post-GD). We found results similar to those obtained in the comparison of the total pre-CA versus post-CA scans. Regardless of the applied contrast material, the EDVi, and ESVi values were significantly larger, while the TMi and PTMi values were significantly smaller when calculated from the post-CA scans (**Figure 11**). Second, we performed these comparisons in the healthy normal group and obtained similar results: the PTMi values were significantly lower in the post-CA scans for both contrast materials. TMi values were also significantly lower in the post-GA scans, and EDVi values were significantly higher in the post-GD scans (**Figure 11**).

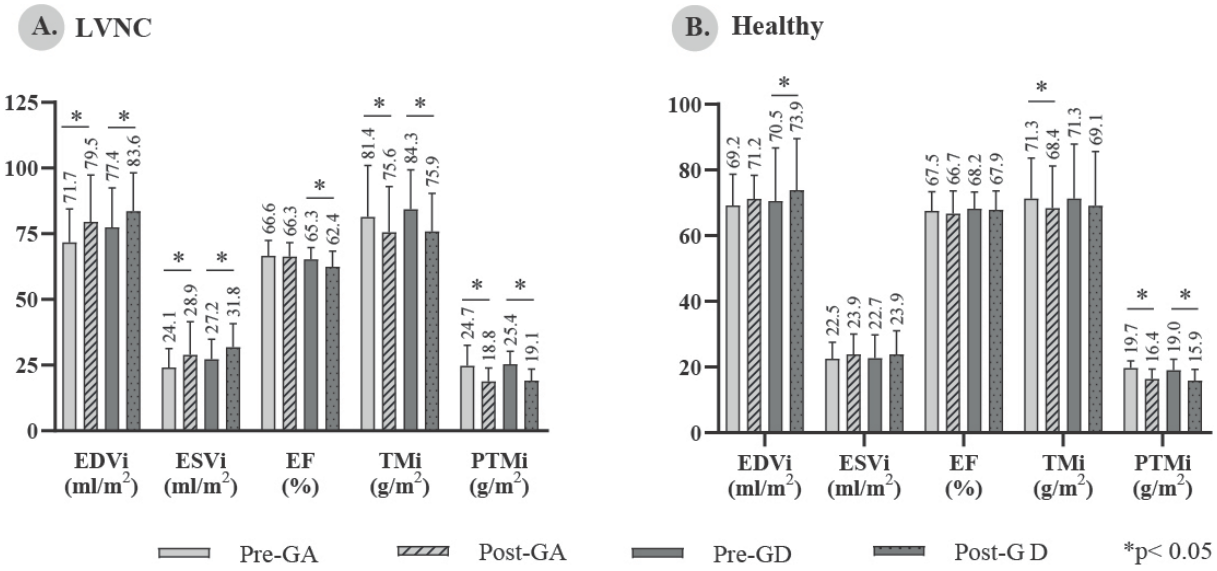

Figure 11. Comparison of the effect of gadobutrol (GA) and gadobenate dimenglumine (GD) on the calculated parameters of left ventricular noncompaction (A) and healthy groups (B).

EDVi: end-diastolic volume index, EF: ejection fraction, ESVi: end-systolic volume index, LVNC: left ventricular noncompaction, post-GA: postgadobutrol, post-GD: postgadobenate dimenglumine, pre-GA: pregadobutrol, pre-GD: pregadobenate dimenglumine, PTMi: end-diastolic papillary and trabeculated myocardial mass index, TMi: end-diastolic total myocardial mass index

Comparison of the contrast agents to each other

Finally, we compared the GA and GD contrast agents to each other in both the healthy and LVNC groups (pre-GA vs. pre-GD, post-GA vs. post-GD). Neither the parameters calculated from the pre-CA scans, nor the ones calculated from the post-CA scans differed significantly in the studied groups **(Figure 12)**.

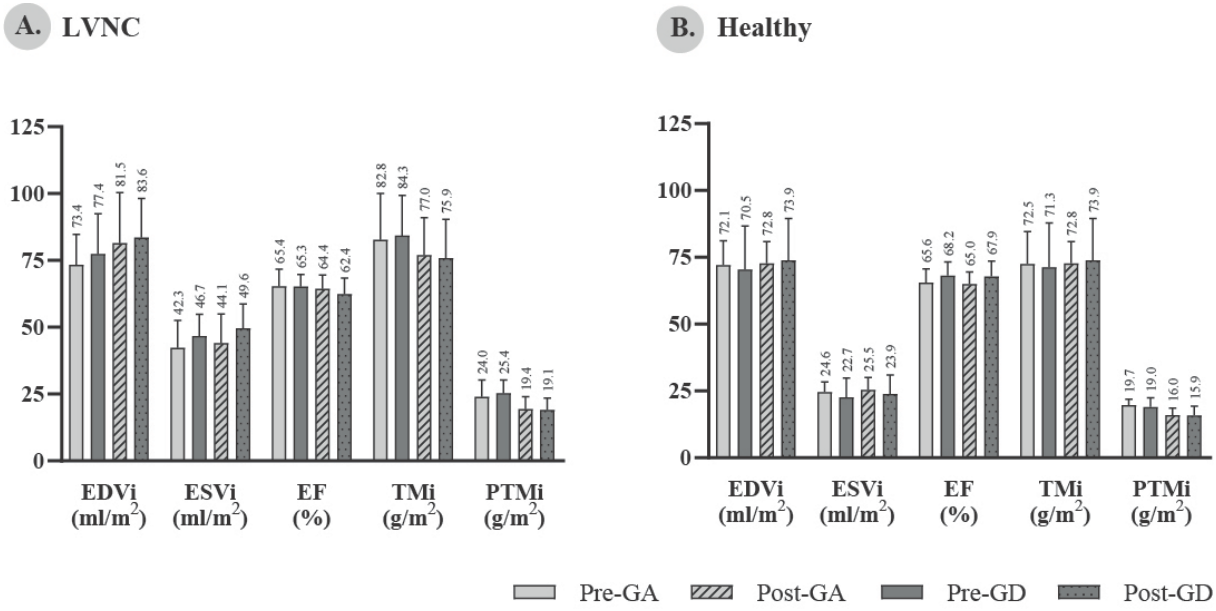

Figure 12. Comparison of the gadobutrol (GA) and gedobenate dimenglumine (GD) receiving left ventricular noncompaction (A) and healthy (B) populations' pre- and postcontrast scans. EDVi: end-diastolic volume index, EF: ejection fraction, ESVi: end-systolic volume index, LVNC: left ventricular noncompaction, post-CA: postcontrast agent, post-GA: postgadobutrol, post-GD: postgadobenate dimenglumine, pre-CA: precontrast agent, pre-GA: pregadobutrol, pre-GD: pregadobenate dimenglumine, PTMi: end-diastolic papillary and trabeculated myocardial mass, TMi: end-diastolic total myocardial mass index

4.2. Results of the left ventricular characteristics of noncompaction phenotype patients with good left ventricular ejection fraction project

Interobserver agreement

We tested the inter-observer agreement on ten randomly selected patients and controls with the interclass correlation coefficient (ICC). Global ICC, which represents the interobserver agreement of all measured LV parameters, was 0.92 (interpreted as: 0.4-0.75 - fair to good, greater than 0.75 - excellent).

The inter-observer agreements of the measured global strain parameters were good-to-excellent: GLS: 0.96 (0.89–0.98), GRS: 0.99 (0.96–0.99), GCS: 0.96 (0.89–0.98), ROT: 0.68 (0.19-0.87), SD-TTP-LS: 0.87 (0.68-0.95), SD-TTP-CS: 0.75 (0.38–0.90).

LV characteristics of patients with LVNC phenotypes and good LV function

First, we compared the LV volumetric, functional and myocardial mass parameters between the LVNC and control groups. The measured parameters in the patients were in the normal range; however, compared with the controls, the LVNC group had significantly higher EDVi, ESVi, TMi, and PTMi values and a significantly lower EF **(Table 3/A)**.

We compared the LV parameters of males and females in both the patient and control groups and found that all the parameters, except the EF, were significantly higher in males than in females **(Table 3/B, 3/C)**.

We also compared male and female LVNC and control groups and found similar results in both sexes. The SVi did not differ between the patients and controls or among males and females **(Table 3/D, 3/E)**.

Table 3. Comparison of left ventricular parameters between LVNC patients and healthy controls, and between sexes.
EDVi: end-diastolic volume index, EF: ejection fraction, ESVi: end-systolic volume index, LVNC: left ventricular noncompaction, PTMi: end-diastolic papillary and trabeculated myocardial mass index, SVi: stroke volume index, TMi: end-diastolic total myocardial mass index

	A.			**B.**			**C.**			**D.**			**E.**		
	Total			LVNC			Control			Male			Female		
	LVNC	Control	p	Male	Female	p	Male	Female	p	LVNC	Control	p	LVNC	Control	p
EDVi (ml/m^2)	77.4±14.5	69.0±11.8	<0.001	83.1±14.3	70.8±11.8	<0.001	73.2±12.2	64.0±9.2	<0.001	83.1±14.3	73.2±12.2	0.001	70.8±11.8	64.0±9.2	0.008
ESVi (ml/m^2)	26.6±7.4	20.6±5.4	<0.001	29.7±7.4	22.9±5.6	<0.001	22.6±5.7	18.2±4.0	<0.001	29.7±7.4	22.6±5.7	<0.001	22.9±5.6	18.2±4.0	<0.001
SVi (ml/m^2)	50.8±9.3	48.8±8.7	0.146	53.4±9.5	47.8±8.1	0.006	50.6±8.7	46.6±8.3	0.037	53.4±9.5	50.6±8.7	0.157	47.8±8.1	46.6±8.3	0.522
EF (%)	65.9±5.2	70.2±5.0	<0.001	64.4±5.1	67.7±4.8	0.004	69.2±5.2	71.5±4.4	0.037	64.4±5.1	69.2±5.2	<0.001	67.7±4.8	71.5±4.4	0.001
TMi (g/m^2)	76.3±17.0	69.7±13.3	0.013	86.8±13.6	64.0±11.5	<0.001	79.3±9.3	58.1±6.4	<0.001	86.8±13.6	79.3±9.3	0.004	64.0±11.5	58.1±6.4	0.016
PTMi (g/m^2)	26.0±7.5	19.4±4.1	<0.001	29.0±7.4	22.4±6.0	<0.001	22.0±3.3	16.4±2.5	<0.001	29.0±7.4	22.0±3.3	<0.001	22.4±6.0	16.4±2.5	<0.001

Cutoff value of the papillary and trabeculated myocardial mass index

By studying the optimal LV-PTMi cutoff values to differentiate between LVNC patients and healthy controls, we found that the optimal cutoffs were 25.8 g/m^2 in males (area under the curve: 0.81, 95% confidence interval: 0.71-0.88, sensitivity: 63.6%, specificity: 93.2%) and 19.0 g/m^2 in females (area under the curve: 0.87, 95% confidence interval: 0.77-0.93, sensitivity: 75.7%, specificity: 89.2%, **Figure 13)**. Participants with a higher LV trabecular mass index value than the proposed cutoffs are more likely to have LVNC than those who are below the described cutoffs.

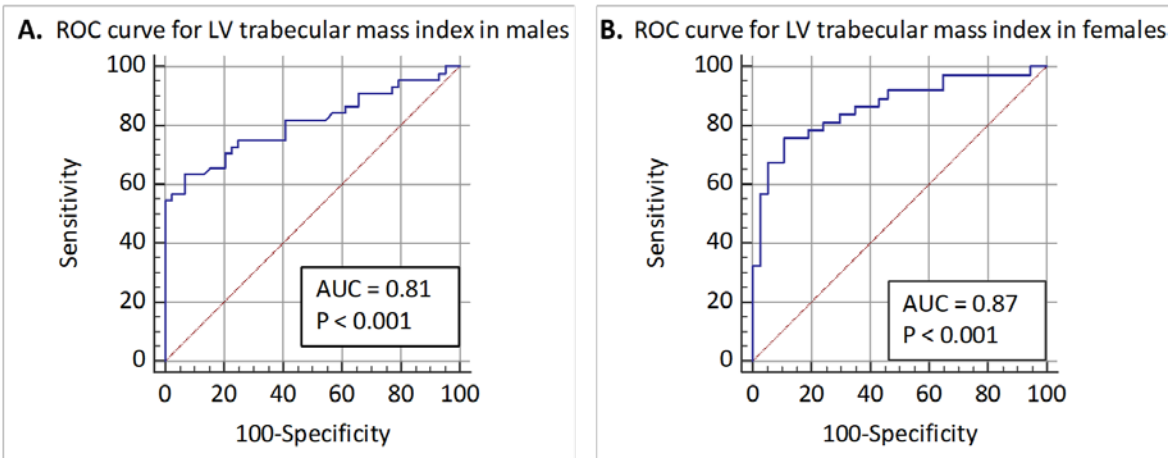

Figure 13. Receiver operating characteristic curves for the trabeculated muscle mass cutoff values in male (A) and female (B) left ventricular noncompaction groups.

LV deformation characteristics of patients with the LVNC phenotype and good LV function

The GCS and GRS in the patient group were significantly worse but still in the normal range, compared with those in the healthy controls, while the GLS and rotation were not significantly different between the two groups. The circumferential mechanical dispersion was significantly higher in the patients than in the controls, while the longitudinal mechanical dispersion was almost equal in the two groups **(Table 4/A)**.

We compared the strain parameters of men and women in the LVNC and control groups, and the GLS was significantly lower for men in both groups than for women. The GRS was also significantly lower in male than in female patients **(Table 4/B, 4/C)**.

By comparing male and female LVNC patients to controls, we found that the GCS and GRS were lower in LVNC patients of both sexes than in male and female healthy controls **(Table 4/D, 4/E)**.

Table 4. Comparison of global strain values between LVNC patients and healthy control groups and between sexes.
GCS: global circumferential strain, GLS: global longitudinal strain, GRS: global radial strain, LVNC: left ventricular noncompaction, ROT: rotation, SD-TTP-CS: standard deviation of time-to-peak circumferential strains, SD-TTP-LS: standard deviation of time-to-peak longitudinal strains

	A.			B.			C.			D.			E.		
	Total			LVNC			Control			Male			Female		
	LVNC	Control	p	Male	Female	p	Male	Female	p	LVNC	Control	p	LVNC	Control	p
GLS (%)	-22.2±2.6	-23.3±3.5	0.155	-21.7±2.7	-22.9±2.4	0.027	-22.7±3.5	-24.0±3.3	0.046	-21.7±2.7	-22.7±3.5	0.125	-22.9±2.4	-24.0±3.3	0.119
GRS (%)	55.6±8.2	64.3±13.2	<0.001	53.8±7.7	57.8±8.4	0.028	63.3±14.2	65.6±12.0	0.276	53.8±7.7	63.3±14.2	0.001	57.8±8.4	65.6±12.0	0.004
GCS (%)	-29.9±4.9	-35.6±4.8	<0.001	-30.3±5.1	-29.5±4.7	0.467	-35.0±4.6	-36.2±5.0	0.29	-30.3±5.1	-35.0±4.6	<0.001	-29.5±4.7	-36.2±5.0	<0.001
ROT (°)	10.1±12.3	7.9±13.4	0.185	12.1±12.1	7.7±13.5	0.127	6.8±15.5	9.2±10.3	0.355	12.1±12.1	6.8±15.5	0.078	7.7±13.5	10.1±30.5	0.589
SD-TTP-LS (%)	10.2±3.9	11.0±3.9	0.178	10.2±4.2	10.3±3.6	0.925	10.9±4.1	11.2±3.7	0.771	10.2±4.2	10.9±4.1	0.398	10.3±3.6	11.2±3.7	0.279
SD-TTP-CS (%)	7.6±4.2	6.1±2.8	0.046	6.8±3.8	8.5±4.6	0.079	5.6±2.7	6.6±2.8	0.075	6.8±3.8	5.6±2.7	0.152	8.5±4.6	6.6±2.8	0.147

4.3. Results of the left ventricular characteristics of patients with left ventricular noncompaction at different deterioration levels of ventricular function project

Interobserver agreement

The interobserver agreement of the two observers was tested regarding the threshold-based software module, the CMR feature-tracking and Petersen's criterion in ten randomly selected patients and ten controls.

The interobserver agreement of the measured LV parameters are as follows: EDVi: 0.98 (0.95–0.99), ESVi: 0.94 (0.84–0 98), SVi: 0.90 (0.75–0.96), EF: 0.76 (0.40–0.91), LV-PTMi: 0.95 (0.86–0.98), and LV-TMi: 0.99 (0.97–0.99). These results are interpreted as follows: less than 0.4 indicates poor, 0.4–0.75 indicates fair to good, and greater than 0.75 indicates excellent. We also measured the interobserver agreement of the noncompacted-to-compacted ratio, which was 0.95 (0.83–0.99).

The interobserver agreement of the measured global strain parameters was also good to excellent: GLS: 0.96 (0.89–0.98), GRS: 0.99 (0.96–0.99), GCS: 0.96 (0.89–0.98), ROT: 0.68 (0.19–0.87), SD-TTP-LS: 0.87 (0.68–0.95), and SD-TTP-CS: 0.75 (0.38–0.90).

LV volumetric, functional and myocardial mass values of the studied groups

In comparisons of the LV volumetric, functional and myocardial mass parameters, we found that Group A had higher volumes, muscle and trabecular muscle mass values and a lower EF than those in the control group. Similar results were found when comparing Group B with Group A and controls. In Group B-1 and Group B-2, the volumes and muscle masses increased and the SVi decreased with the decrease in EF **(Table 5)**. Late gadolinium enhancement with a nonischemic midmyocardial pattern was present in 5 patients in Group B-1 and in 11 patients in Group B-2.

Global strain parameters of the studied groups

We compared the global strain parameters of Group B with those of Group A and controls. The GLS, GRS and GCS were significantly worse (i.e., GLS and GCS were less negative and GRS was less positive) in Group B than in Group A and in the controls, and the GCS and GRS were also significantly worse in Group A than in the controls **(Table 5)**.

After dividing Group B into two subgroups, we found that all the global strain parameters differed significantly among Groups A, B-1, and B-2. Specifically, a worse EF was associated with worse strain parameters **(Table 5)**.

Table 5. Left ventricular functional, global strain, mechanical dispersion and rotational values of the studied groups.
EDVi: end-diastolic volume index, EF: ejection fraction, ESVi: end-systolic volume index, GCS: global circumferential strain, GLS: global longitudinal strain, GRS: global radial strain, LVNC: left ventricular noncompaction, PTMi: end-diastolic papillary and trabeculated myocardial mass index, SD-TTP-CS: standard deviation of time-to-peak circumferential strains, SD-TTP-LS: standard deviation of time-to-peak longitudinal strains, SVi: stroke volume index, TMi: end-diastolic total myocardial mass index

						p value					
	Control	Group A LVNC EF>50%	Group B LVNC EF<50%	Group B-1 LVNC EF 35-50%	Group B-2 LVNC EF<35%	Group A vs. Control	Group B vs. Control	Group B vs. Group A	Group B-1 vs. Group A	Group B-2 vs. Group A	Group B-2 vs. Group B-1
Number of participants (male)	31 (21)	31 (21)	31 (21)	13 (8)	18 (13)	-	-	-	-	-	-
EDVi (ml/m2)	66.4±12.6	72.0±12.5	121.8±38.5	92.9±13.0	142.6±37.5	0.782	<0.0001	<0.0001	<0.0001	<0.0001	<0.0001
ESVi (ml/m2)	19.5±4.9	25.4±6.7	84.4±36.1	53.0±9.1	107.1±30.8	0,044	<0.0001	<0.0001	<0.0001	<0.0001	<0.0001
SVi (ml/m2)	46.8±8.8	46.6±7.6	37.3±9.1	39.9±5.7	35.5±10.7	0.996	<0.0001	<0.0001	0.131	<0.0001	0.302
EF (%)	70.6±4.2	65.0±5.1	32.8±10.1	43.1±4.1	25.3±5.3	<0.0001	<0.0001	<0.0001	<0.0001	<0.0001	<0.0001
TMi (g/m2)	71.7±13.8	80.9±18.9	123.2±29.4	98.5±19.0	141.0±21.6	0.079	<0.0001	<0.0001	0,025	<0.0001	<0.0001
PTMi (g/m2)	20.0±4.1	28.4±8.4	48.2±13.2	38.9±9.3	55.0±11.5	<0.0001	<0.0001	<0.0001	0,006	<0.0001	<0.0001
GLS (%)	-22.9±2.5	-21.7±2.5	-10.4±3.9	-13.9±2.6	-8.0±2.6	0.132	<0.0001	<0.0001	<0.0001	<0.0001	<0.0001
GRS (%)	62.3±9.2	55.2±8.2	20.2±8.0	28.2±4.0	14.5±4.1	0,004	<0.0001	<0.0001	<0.0001	<0.0001	<0.0001
GCS (%)	-35.0±4.2	-31.0±4.9	-11.0±6.2	-16.1±3.4	-7.3±5.0	0,003	<0.0001	<0.0001	0,001	<0.0001	0,048
Apical rotation (◦)	10.1±12.6	10.1±8.7	0.1±5.7	3.4±5.4	-2.2±5.7	1.000	0,001	<0.0001	0,019	<0.0001	0.101
Basal rotation (◦)	0.4±8.8	-0.1±6.5	-3.5±4.2	-4.6±4.3	-3.1±3.9	0.973	0.087	0,048	0,041	0,159	0.740
SD-TTP-LS (%)	12.2±4.1	10.9±4.4	15.9±4.5	14.0±4.4	17.2±4.1	0.485	0,003	<0.0001	0,089	<0.0001	0.101
SD-TTP-CS (%)	6.9±3.4	7.6±4.6	15.8±5.3	13.9±5.8	17.2±4.5	1.000	<0.0001	<0.0001	0,004	<0.0001	0.621

Differences in mean segmental strain values between the studied groups

A comparison of the mean longitudinal strain values of the apical, mid and basal parts of the LV among the groups showed that compared with Group A and the controls, Group B had significantly worse longitudinal strain values in every part of the LV. These parameters did not differ between Group A and the controls. Comparisons of Group B-1 and Group B-2 with each other and with Group A showed that the longitudinal strain values were significantly different between these groups in each part of the LV **(Table 6)**.

Similar results were found when comparing the mean segmental circumferential strain values of the studied groups **(Table 6)**.

Table 6. Comparison of the mean apical, mid and basal left ventricular longitudinal and circumferential strain values of the studied groups.
EF: ejection fraction, LVNC: left ventricular noncompaction

Longitudinal strain (%)	Control	Group A LVNC EF>50%	Group B LVNC EF<50%	Group B-1 LVNC EF 35-50%	Group B-2 LVNC EF<35%	p value					
						Group A vs. Control	Group B vs. Control	Group B vs. Group A	Group B-1 vs. Group A	Group B-2 vs. Group A	Group B-2 vs. Group B-1
Apical	-23.3±4.4	-22.5±5.7	-11.4±4.1	-14.2±4.1	-9.3±2.8	0.764	<0.0001	<0.0001	<0.0001	<0.0001	0.015
Mid	-24.9±4.9	-24.0±4.5	-14.2±4.1	-17.3±3.7	-11.9±2.8	0.712	<0.0001	<0.0001	<0.0001	<0.0001	0.001
Basal	-22.3±3.3	-21.2±4.4	-13.6±4.4	-16.2±3.8	-11.7±4.0	0.570	<0.0001	<0.0001	0.002	<0.0001	0.012
Circumferential strain (%)											
Apical	-41.4±6.7	-34.3±10.4	-15.2±5.6	-19.3±5.3	-12.3±3.8	0.007	<0.0001	<0.0001	<0.0001	<0.0001	0.002
Mid	-28.6±4.4	-25.1±3.6	-13.0±3.9	-16.7±2.6	-10.4±2.0	0.002	<0.0001	<0.0001	0.001	<0.0001	0.043
Basal	-34.4±3.2	-31.1±4.5	-15.1±4.7	-19.1±4.2	-12.2±2.4	0.143	<0.0001	<0.0001	0.001	<0.0001	0.056

Mean segmental strain values of the studied groups

In studying the mean apical, mid and basal LV longitudinal strain values in each group, we found that the LV mid part had the highest (i.e., more negative) strain value in every group. The basal part had the lowest (i.e., less negative) longitudinal strain values out of the three parts of the LV in Group A and in the controls, while the lowest values were found in the apical part of the LV in Groups B, B-1, and B-2 **(Figure 14)**.

Regarding the mean circumferential strains, we found significant differences among the apical, mid and basal LV strain values in Group A and the controls but not in Group B or its subgroups. The mean strain values were decreased in every part of the LV in Group B and its B-1 and B-2 subgroups; however, the strain pattern remained the same, opposing the mean longitudinal strains where the pattern changed with the decrease in EF **(Figure 14)**.

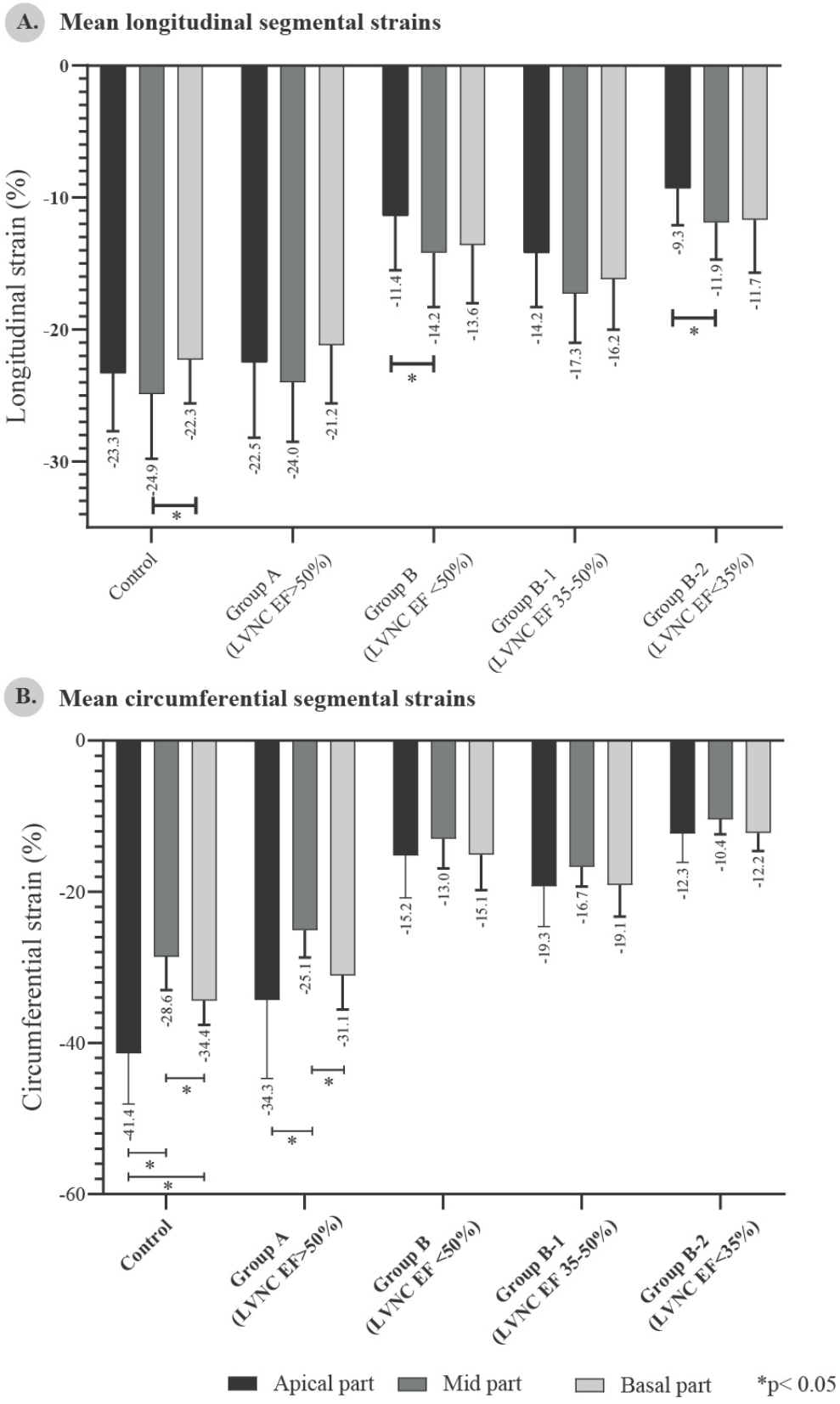

Figure 14. Comparison of the mean apical, mid and basal left ventricular longitudinal (A) and circumferential (B) strain values in each group.

EF: ejection fraction, LVNC: left ventricular noncompaction

Mechanical dispersion

The mechanical dispersion in both the longitudinal (SD-TTP-LS) and circumferential (SD-TTP-CS) directions was significantly higher in Group B than in Group A and in the controls, and there was no significant difference between the two groups. Regarding the B-1 and B-2 subgroups, the mechanical dispersion increased in both directions as EF decreased **(Table 5)**.

Rotational pattern

The degree of peak apical rotation was almost equal between Group A and the controls, and it significantly decreased as EF decreased. Notably, the direction of apical rotation was reversed in Group B-2. The basal rotation was significantly different between Group A and Group B; however, after dividing Group B, we found that the difference was significant only between Group B-1 and Group B-2 **(Table 5)**.

In studying the LV rotational patterns of the LVNC and control groups, we found that RBR occurred in 42% of the patients in Group B (Group B-2: n=10, Group B-1: n=3), in whom the rotational patterns were clockwise-directed in a majority of the cases (Group B-2: n=10, Group B-1: n=2). Twenty-six percent of the patients in Group A also had RBR (n=8); however, almost all of these patients showed counterclockwise RBR (n=7). Surprisingly, 23% (n=7) of the control subjects also had a counterclockwise-directed RBR.

5. Discussion

5.1. Discussion of the effect of contrast agent on left ventricular parameters using a threshold-based software module

CMR imaging is currently the gold standard for measuring cardiac volume and function and myocardial mass (71-74). In recent years, an increasing number of postprocessing programs have been equipped with threshold-based papillary and trabeculated muscle-quantifying algorithms, leading to an easier and faster evaluation with excellent reproducibility, and more accurate cardiac volumes, and masses (55, 75).

We studied the effect of contrast agents on the applicability of threshold-based papillary and trabeculated myocardial mass quantification software in patients with LVNC and in healthy normal study subjects.

Our results showed that the LV end-diastolic and end-systolic volumes calculated from post-CA scans were significantly higher, while the total and trabeculated myocardial mass values calculated from post-CA scans were significantly lower than those calculated from pre-CA images in both the LVNC and healthy normal groups. However, the difference between the pre-CA and post-CA parameters was significantly larger in the patient group than in the healthy group.

The signal intensity of SSFP images depends on the T2/T1 ratio of the tissue of interest. Gadolinium-based extracellular contrast agents decrease the T1 values of blood and myocardial tissue, which results in an increased signal intensity on SSFP images. This effect is more pronounced in the myocardium and less pronounced in the blood pool, leading to decreased contrast between the two tissues. T2 values are slightly reduced by contrast agents administered at low doses (0.1-0.3 mmol/kg), and these changes are overridden by T1 shortening; thus, changes in the signal intensity after administration of a contrast agent are due to changes in T1 values (76-78). The end result of these changes in relaxivity is that the difference between the T1/T2 ratios of the blood and the myocardium decreases after contrast administration. As the mechanism of threshold-based quantification is based on the high signal intensity difference between the blood and the myocardium, our results suggest that this effect has a significant impact on the detection of endocardial trabeculae on postcontrast scans, not only in patients with LV hypertrabeculation but also in patients with normal trabeculation. Our results correlate with those from a study about the precision of feature-tracking techniques from a different vendor on post-CA scans. In that study, contrast agent significantly changed the measured strain values, which also confirmed the importance of the signal intensity-altering effect of contrast

agents (64). These results are important both during regular CMR postprocessing and in research projects for standardizing protocols.

We also studied the effect of two different contrast materials on the precision of threshold-based software to determine whether the change in the calculated parameters depends on the type of contrast agent applied. The trabeculated myocardial mass value was significantly smaller and the end-diastolic volume was larger on both postgadobutrol and postgadobenate dimenglumine images. However, no significant differences were found in the comparison between the two contrast agents.

Gadolinium is a paramagnetic extracellular contrast agent that shortens the T1 and T2 relaxation time of the surrounding protons, which increases the signal intensity on T1-weighted images (79). Different chelators are used to create complexes with gadolinium; therefore, different products are available. Compared with traditional extracellular gadolinium contrast agents, gadobenate dimenglumine binds weakly to albumin and attenuates the signal intensity of blood, has a slight intravascular effect and prolongs the plasma half-life. Gadobutrol does not bind to proteins but reduces T1 values more than gadobenate dimenglumine because of its concentration (80-82). These properties do not seem to make a significant difference regarding the effect studied herein. However, as the altering effect of contrast agent on the calculated parameters was independent of the type of contrast material applied, the method of evaluation should be standardized.

I would like to mention the main limitation of this study, namely, this was a single-center study, and the number of included participants were small.

5.2. Discussion of the left ventricular characteristics of noncompaction phenotype patients with good ejection fraction project

In this retrospective study, we described the LV characteristics of a large cohort who fulfilled the morphological criteria of LVNC and had a good LV ejection fraction, and we evaluated the differences between male and female patients.

The volumetric and myocardial mass values were in the normal range; however, the LVNC group had significantly larger end-systolic and end-diastolic volumes and a significantly smaller ejection fraction than the control group. These results correlate with those presented by Zemrak et al., who described in a population free of clinically recognized cardiovascular disease that a higher LV trabeculated muscle/total myocardial mass ratio is associated with a lower LV ejection fraction and higher LV volumes (13). However, no association was found between increased LV trabeculation and an increase in LV volumes or a decrease in LV function during

the 9.5-year follow-up of the same study population (16). Another study also revealed that the morphological diagnosis of LVNC itself was not associated with adverse clinical events during almost 7 years of follow-up (83). These results suggest that the noncompaction phenotype itself does not result in LV dysfunction over time. Thus, the diagnosis of LVNC based exclusively on morphological criteria might be insufficient, and an integrated diagnostic algorithm with additional anamnestic and clinical information should be used to avoid overdiagnosis (84).

Well-known biometric alterations between sexes were present in our male and female control groups, and these alterations could be the cause of significant differences between the volumetric and functional parameters of male and female LVNC patients (9). Previous studies using other techniques have described the different trabeculated volumes and the different thicknesses but not the differing trabeculated muscle mass of noncompacted and compacted myocardium between healthy males and females, as we did in the present study (9). Furthermore, our results showed that the optimal trabecular mass index cutoff value for LVNC was markedly different in men compared with women, suggesting that the diagnostic cutoffs should be sex-specific. The LV trabecular mass index might be a useful parameter, but further studies are required, as the sensitivities of the proposed cutoff values were quite low in our study. Grothoff et al. previously proposed a cutoff value for noncompacted myocardial mass index regardless of sex of 15 g/m^2, although their study included a smaller LVNC population, and they used a different method to measure trabeculated myocardium mass (42).

Of the studied feature-tracking strain parameters, GLS was not different between the LVNC group and the controls in our study. The normal GLS value in addition to the good ejection fraction suggests normal LV function and no presence of subtle LV dysfunction in this patient cohort. In contrast to our results, a recent publication described a decreased GLS in patients with LVNC with a median LV ejection fraction of 54%, which is lower than the mean ejection fraction found in our LVNC group (85). We know from mathematical and echocardiographic studies that for patients with an LV ejection fraction higher than 50%, the GLS can vary more with less effect on ejection fraction than in patients with a decreased LV function, which could explain these diverse results (86). The GLS values in male patients and male controls were significantly reduced (but still in the normal range) compared with those in female patients and controls, which seems to be a sex-related difference rather than an LVNC-related phenomenon (87, 88).

In contrast to GLS, the GCS and GRS values in LVNC patients were significantly reduced compared with the controls, and this significance did not change after we stratified the groups by sex. These results correlate with the findings of a recent study on a pediatric LVNC

population with a good ejection fraction, although this was performed with speckle tracking echocardiography (89). Cardiac magnetic resonance studies on healthy populations showed that an increase in LV trabeculation was associated with impaired circumferential strain, even after adjustments for age, sex and body mass index; however, the relationship between LV hypertrabeculation and decreased circumferential strain was unclear (7, 90). In addition to decreased GCS, circumferential mechanical dispersion, which describes interventricular desynchrony, was higher in patients than in controls. We do not have enough information yet to evaluate the clinical relevance of this statistically significant result because feature-tracking normal values for the standard deviation of time-to-peak circumferential strain are not available. In previous studies conducted using healthy populations, mechanical dispersion was higher in participants with a longer QTc time, and mechanical dispersion was also predictive of arrhythmic risk in different diseases (91-94). Further follow-up studies are necessary to investigate the possible prognostic role of these parameters in this patient population.

Regarding the changes in GRS, radial thickening arises from both longitudinal and circumferential shortening; thus, compared with that in controls, the significantly decreased GRS value in patients may be due to the significantly decreased GCS. The difference in GRS between male and female patients may be due to the small numbers of patients when we separated the groups by sex. The GRS is less reproducible than the other two global strain parameters and shows large differences among studies regarding a normal range; thus, the importance of the GRS requires further evaluation (87, 95, 96).

We would like to mention the limitations of this study. Unfortunately, detailed clinical information (ECG, symptoms, genetic test result) was not available for the included LVNC patients. Regarding the threshold-based software program, the current ejection fraction and volume quantification uses a stack of thick short-axis slices, and 8 mm is common for Z-direction spatial resolution. Moreover, trabeculae and papillary muscles do not cross the slice in an exactly perpendicular fashion, which creates partial volume effects. Depending on the actual path of the trabeculae, this feature will influence the threshold-based quantification (53, 56). Furthermore, altering the threshold might change the measured myocardial mass values.

We would also like to mention some limitations of the feature-tracking method. This method lacks a relevant validation process; thus, its clinical application is questionable. The reproducibility of segmental strain is worse than that of the other acquisition-based techniques; thus, we must to be careful when evaluating LV regional dysfunction with feature tracking.

There is high variability in normal strain values between different vendors, and there is a lack of an accepted normal reference range (57, 60).

5.3. Discussion of the left ventricular characteristics of patients with left ventricular noncompaction at different deterioration levels of ventricular function project

In this study, we described the LV global and segmental CMR FT strain characteristics of LVNC patients on the spectrum of a good to a severely reduced LV ejection fraction.

The LVNC patients with reduced LV function had a remodeled LV with higher volumes, higher myocardial and trabecular masses and a lower SVi than LVNC patients with good LV function. These alterations correlate with previous studies describing the echocardiography and CMR features of LVNC patients with impaired systolic function, while an increased trabeculated muscle mass is characteristic of the disease (97, 98). The functional parameters of LVNC patients with a good LV ejection fraction compared with the healthy control participants were in the normal range, but the volumes and masses were higher, while the EF was lower. These findings are in accordance with our results described in Section 4.2 and discussed in Section 5.2, and they may be related to the presence of excessive endocardial trabeculation (99). The clinical relevance of these volumetric and functional alterations is still unknown, and they should be evaluated together with the patient's symptoms, ECG findings, and medical history (24).

The LV is composed of a complex three-layered myocardial structure that leads to longitudinal, circumferential and radial-directed deformation of the myocardium (58). It is already known that LV global strains strongly correlate with EF; thus, the worsening of LV function is associated with a decrease in LV global strain parameters (86, 100, 101). In our study, we found that the GLS, GCS and GRS gradually decreased as LV function worsened. The decreased strains in all three directions suggest that LVNC is a complex structural disease that affects not only the noncompacted but also the compacted layer (102, 103).

Regarding LVNC patients with good LV function, their GLS was not different from that of the control group, which is in accordance with the results of Gastl et al. (104). However, this finding may be controversial, as other researchers have observed impaired GLS in both adult and pediatric LVNC patient populations despite good LV function (105, 106). These conflicting results could be due to the nonlinear relationship between LV ejection fraction and GLS described earlier, namely, there is a stronger correlation between these two parameters at a lower EF, and the curve flattens when the EF is higher than 50%. Thus, in the latter case, GLS can vary more with a reduced effect on LV EF (86, 101).

GCS and GRS were significantly worse in patients with a good LV EF than in controls, but they were still in the normal range. Other researchers have found similar results in pediatric patients and lower than normal GCS values in adult LVNC patients with good LV function (89, 104). However, decreased GCS and GRS values were also present in healthy participants with LV hypertrabeculation, and Cai et al. described an independent association of higher global fractal dimension values with decreased GCS after adjusting for age, sex and body mass index (90, 107). This result raises the question of whether the presence of LV hypertrabeculation causes this alteration or whether subclinical LV dysfunction is already present in LVNC patients regardless of having good LV function. Follow-up studies with a large number of included LVNC patients should help to address this question, as neither the pathomechanism nor its clinical relevance has been determined.

In studying the mean segmental strain values of the apical, mid and basal regions, we found an increase in segmental strain values from base to apex, which has been previously described in healthy adults; however, our results were slightly different, namely, the mid part had the best longitudinal strain value, which could be due to the small number of included patients (108). Previous CMR and speckle-tracking echocardiography studies have mentioned that these regional strain differences disappear in patients with DCM, and in accordance with this conclusion, we also observed that the decrease in segmental strains affected all three parts of the LV in LVNC patients with a reduced EF (102, 109). Furthermore, an opposite pattern was exhibited in this LVNC patient group; namely, apical longitudinal strain became the worst of the three parts, which was previously described in different DCM and LVNC populations with a severely reduced EF (110, 111). Niemann et al. compared LVNC patients with a reduced EF to DCM patients with speckle-tracking echocardiography and found decreased apical strains in both groups; moreover, Tufekcioglu also found similar contraction properties between patients with LVNC and DCM (45, 112). Together with the evenly decreased circumferential segmental strain values, these results suggest that the regional strain patterns in LVNC are very similar to those described in DCM and are not specific to noncompaction as an etiological factor of heart failure. However, opposing results regarding apical strain in the LVNC can be found in the literature, which might be due to the different strain measurement techniques and the different vendors (46). Furthermore, the lack of an LVNC-specific pattern might be due to the small sample size in our study, and the presence of LVNC-specific signs and patterns cannot be excluded.

In addition to the advantages of feature tracking, such as the postprocessing nature and the excellent reproducibility and correlation of global strains with both the gold-standard tagging

and fast-strain encoded MRI methods (fast-SENC), we need to mention some disadvantages that might play a role in the inability to describe any LVNC-specific strain pattern (60). The intraobserver and interstudy agreement for segmental strains seem to be the worst in feature tracking when compared with tagging and fast-SENC; furthermore, the reproducibility is highly dependent on the observer's experience (57, 60, 113). This phenomenon may have affected our regional strain results; however, we tried to reduce its effect by taking the average values of the LV thirds.

Mechanical dispersion (SD-TTP-CS and SD-TTP-LS) increased in both the longitudinal and circumferential directions as EF decreased, a pattern characteristic of DCM according to echocardiographic studies; however, when measured with CMR, this parameter had a smaller background (114, 115).

The apical rotation value was significantly smaller in the patients with a reduced EF than in the patients with a good EF or the controls, and after dividing the patients by the EF, apical rotation decreased as LV function worsened. Furthermore, the direction of apical rotation was reversed in patients with severely decreased LV function (Group B-2). Kim et al., using speckle-tracking echocardiography, demonstrated that the LV EF is correlated with the degree of apical rotation but not with the degree of basal rotation. Moreover, Popescu et al. suggested that a decrease in apical rotation is related to LV dilation and increased sphericity and reflects a more advanced disease stage, in accordance with our findings (116, 117). The lack of difference between the patients with good EF and healthy controls also strengthens this phenomenon. We found only a few significant results regarding basal rotation, perhaps because of the heterogeneous basal rotation values and the small number of included patients. Additionally, the importance of basal rotation has been less well studied than the role of apical rotation in the LV EF, as described above.

LV rigid body rotation has been mentioned in previous papers as a characteristic rotation pattern in LVNC; however, it has also been demonstrated in several other disorders, e.g., dilated and hypertensive cardiomyopathy, amyloidosis or different types of congenital heart diseases (47, 118-120). In our study population, a mainly clockwise-directed RBR was found in the patients with a reduced EF. Some studies have shown that patients with a clockwise RBR have higher volumes and more severely reduced EF and LV remodeling, which leads to a decrease in apical rotation and can eventually result in reversed apical rotation and clockwise RBR (116, 118, 121, 122). These findings are in accordance with our own results. Interestingly, a counterclockwise RBR was more characteristic of LVNC patients with a good EF, and it was present in almost a quarter of the control patients as well. This type of RBR was found to be a

normal pattern in healthy infants, but the cause and importance of this alteration in healthy adults and LVNC patients with good LV function remains unclear (123). We would like to highlight that RBR has mostly been studied with speckle-tracking echocardiography; thus, further research on the role and reproducibility of CMR strain measurement software is needed. The limitations of this study arise from the small number of included patients, and from the previously described limitations of the threshold-based software program and the feature-tracking method.

6. Conclusions

Left ventricular noncompaction is a widely studied entity with suboptimal morphologic criteria and controversial data on the myocardial mechanics of the hypertrabeculated LV.

In our first CMR study, we raised the question of whether administration of contrast agent before the acquisition of bSSFP cine images had an effect on the calculated parameters using a threshold-based postprocessing algorithm and whether these effects are more pronounced in patients with LV hypertrabeculation. Our prospective study revealed that threshold-based papillary and trabeculated myocardial mass quantifying software provides altered results when short-axis scans are performed after the injection of contrast material, as the signal intensity difference between the blood and the myocardium is decreased on these postcontrast images. Contrast agents influenced the measured values, especially in patients with excessive endocardial trabeculation, and this effect was independent of the type of contrast agent applied; therefore, the method of evaluation should be standardized.

In the second part of our study, we retrospectively analyzed the CMR functional and strain parameters of a large cohort, which fulfilled the morphologic criteria for LVNC and had good LV function, and we searched for sex-specific differences. All the measured parameters were in the normal range but differed significantly from those of healthy controls, which might be caused by the increased amount of LV trabeculation. The decreased GCS and GRS values and increased circumferential mechanical dispersion could also be related to excessive trabeculation. The LV trabeculated muscle mass is highly different in males and females; thus, the use of sex-specific morphologic diagnostic criteria should be considered.

Finally, we described the changes in strain parameters at different deterioration levels of LV function. The strain values and rotational parameters gradually worsened as EF decreased in patients with LVNC. In this study, we could not identify a pattern specific to LVNC; however, we cannot exclude its existence. For this reason, further prospective studies with larger numbers of patients are needed.

7. Summary

LVNC is a rare disease with excessive endomyocardial trabeculation in the apical part of the LV. In many cases, it is an incidental finding in asymptomatic patients with good LV function; however, LVNC can manifest as severe heart failure and dilated cardiomyopathy (84). Developments in imaging technology have improved the visualization of ventricular trabeculation, and CMR is the recommended diagnostic modality with several diagnostic criteria in the field (22). However, standardized protocols, including acquisition and postprocessing, are not available for the assessment of trabeculated myocardium.

The goal of our first, prospective study was to study the applicability of threshold-based papillary and trabeculated muscle quantification software on bSSFP cine images acquired after the injection of contrast agent. We have confirmed that the abovementioned software provides altered results when bSSFP cine scans are performed after the injection of contrast material, as the signal intensity difference is decreased on these postcontrast images. The alteration between pre- and postcontrast results was greater in patients with LV hypertrabeculation/noncompaction; however, it was also present in healthy participants, and this effect was independent of the type of the applied contrast material. Thus, we suggest that short-axis cine images used for volumetric and functional assessments should be taken before the administration of contrast material in patients with excessive LV trabeculation.

It is still not clear whether all subjects with LVNC have cardiomyopathy. Novel imaging modalities, such as deformation analysis, may help differentiate a normal anatomic phenotype and LVNC cardiomyopathy with new diagnostic and prognostic parameters. However, the results are controversial, and CMR FT analysis has not been used previously. Thus, we retrospectively analyzed the CMR images of patients with LVNC with the aim of describing their LV characteristics, to investigate sex-specific cutoff points of LV trabeculated muscle mass and to describe the changes in strain parameters at different deterioration levels of LV function. The LV volumetric, functional and strain parameters of LVNC patients differed significantly from those of healthy controls, which might be related to the presence of excessive LV trabeculation. We demonstrated that LV trabeculated muscle mass greatly differed between sexes; thus, the use of sex-specific morphologic diagnostic criteria should be considered. The strain values and rotational parameters gradually worsened as EF decreased; however, we could not identify a pattern specific to LVNC. Despite this, we cannot exclude its existence, and further prospective studies with larger numbers of patients are needed to evaluate this possibility.

8. References

1. Sedmera D, Pexieder T, Vuillemin M, Thompson RP, Anderson RH. (2000) Developmental patterning of the myocardium. Anat Rec, 258: 319-337.
2. Captur G, Syrris P, Obianyo C, Limongelli G, Moon JC. (2015) Formation and Malformation of Cardiac Trabeculae: Biological Basis, Clinical Significance, and Special Yield of Magnetic Resonance Imaging in Assessment. Can J Cardiol, 31: 1325-1337.
3. Zhang W, Chen H, Qu X, Chang CP, Shou W. (2013) Molecular mechanism of ventricular trabeculation/compaction and the pathogenesis of the left ventricular noncompaction cardiomyopathy (LVNC). Am J Med Genet C Semin Med Genet, 163C: 144-156.
4. Paun B, Bijnens B, Butakoff C. (2018) Relationship between the left ventricular size and the amount of trabeculations. Int J Numer Method Biomed Eng, 34.
5. Bentatou Z, Finas M, Habert P, Kober F, Guye M, Bricq S, Lalande A, Frandon J, Dacher JN, Dubourg B, Habib G, Caudron J, Normant S, Rapacchi S, Bernard M, Jacquier A. (2018) Distribution of left ventricular trabeculation across age and gender in 140 healthy Caucasian subjects on MR imaging. Diagn Interv Imaging, 99: 689-698.
6. Chuang ML, Gona P, Hautvast GL, Salton CJ, Blease SJ, Yeon SB, Breeuwer M, O'Donnell CJ, Manning WJ. (2012) Correlation of trabeculae and papillary muscles with clinical and cardiac characteristics and impact on CMR measures of LV anatomy and function. JACC Cardiovasc Imaging, 5: 1115-1123.
7. Cai J, Bryant JA, Le TT, Su B, de Marvao A, O'Regan DP, Cook SA, Chin CW. (2017) Fractal analysis of left ventricular trabeculations is associated with impaired myocardial deformation in healthy Chinese. J Cardiovasc Magn Reson, 19: 102.
8. Choi Y, Kim SM, Lee SC, Chang SA, Jang SY, Choe YH. (2016) Quantification of left ventricular trabeculae using cardiovascular magnetic resonance for the diagnosis of left ventricular non-compaction: evaluation of trabecular volume and refined semi-quantitative criteria. J Cardiovasc Magn Reson, 18: 24.
9. Andre F, Burger A, Lossnitzer D, Buss SJ, Abdel-Aty H, Gianntisis E, Steen H, Katus HA. (2015) Reference values for left and right ventricular trabeculation and non-compacted myocardium. Int J Cardiol, 185: 240-247.
10. Gregor Z, Kiss AR, Szabo LE, Toth A, Grebur K, Horvath M, Dohy Z, Merkely B, Vago H, Szucs A. (2021) Sex- and age- specific normal values of left ventricular

functional and myocardial mass parameters using threshold-based trabeculae quantification. PLoS One, 16: e0258362.

11. Petersen SE, Selvanayagam JB, Wiesmann F, Robson MD, Francis JM, Anderson RH, Watkins H, Neubauer S. (2005) Left ventricular non-compaction: insights from cardiovascular magnetic resonance imaging. J Am Coll Cardiol, 46: 101-105.
12. Jenni R, Oechslin E, Schneider J, Attenhofer Jost C, Kaufmann PA. (2001) Echocardiographic and pathoanatomical characteristics of isolated left ventricular non-compaction: a step towards classification as a distinct cardiomyopathy. Heart, 86: 666-671.
13. Kawel N, Nacif M, Arai AE, Gomes AS, Hundley WG, Johnson WC, Prince MR, Stacey RB, Lima JA, Bluemke DA. (2012) Trabeculated (noncompacted) and compact myocardium in adults: the multi-ethnic study of atherosclerosis. Circ Cardiovasc Imaging, 5: 357-366.
14. Captur G, Zemrak F, Muthurangu V, Petersen SE, Li C, Bassett P, Kawel-Boehm N, McKenna WJ, Elliott PM, Lima JA, Bluemke DA, Moon JC. (2015) Fractal Analysis of Myocardial Trabeculations in 2547 Study Participants: Multi-Ethnic Study of Atherosclerosis. Radiology, 277: 707-715.
15. Weir-McCall JR, Yeap PM, Papagiorcopulo C, Fitzgerald K, Gandy SJ, Lambert M, Belch JJ, Cavin I, Littleford R, Macfarlane JA, Matthew SZ, Nicholas RS, Struthers AD, Sullivan F, Waugh SA, White RD, Houston JG. (2016) Left Ventricular Noncompaction: Anatomical Phenotype or Distinct Cardiomyopathy? J Am Coll Cardiol, 68: 2157-2165.
16. Zemrak F, Ahlman MA, Captur G, Mohiddin SA, Kawel-Boehm N, Prince MR, Moon JC, Hundley WG, Lima JA, Bluemke DA, Petersen SE. (2014) The relationship of left ventricular trabeculation to ventricular function and structure over a 9.5-year follow-up: the MESA study. J Am Coll Cardiol, 64: 1971-1980.
17. Gati S, Chandra N, Bennett RL, Reed M, Kervio G, Panoulas VF, Ghani S, Sheikh N, Zaidi A, Wilson M, Papadakis M, Carre F, Sharma S. (2013) Increased left ventricular trabeculation in highly trained athletes: do we need more stringent criteria for the diagnosis of left ventricular non-compaction in athletes? Heart, 99: 401-408.
18. Gati S, Papadakis M, Papamichael ND, Zaidi A, Sheikh N, Reed M, Sharma R, Thilaganathan B, Sharma S. (2014) Reversible de novo left ventricular trabeculations in pregnant women: implications for the diagnosis of left ventricular noncompaction in low-risk populations. Circulation, 130: 475-483.

19. de la Chica JA, Gomez-Talavera S, Garcia-Ruiz JM, Garcia-Lunar I, Oliva B, Fernandez-Alvira JM, Lopez-Melgar B, Sanchez-Gonzalez J, de la Pompa JL, Mendiguren JM, Martinez de Vega V, Fernandez-Ortiz A, Sanz J, Fernandez-Friera L, Ibanez B, Fuster V. (2020) Association Between Left Ventricular Noncompaction and Vigorous Physical Activity. J Am Coll Cardiol, 76: 1723-1733.
20. D'Ascenzi F, Pelliccia A, Natali BM, Bonifazi M, Mondillo S. (2015) Exercise-induced left-ventricular hypertrabeculation in athlete's heart. Int J Cardiol, 181: 320-322.
21. Arbustini E, Weidemann F, Hall JL. (2014) Left ventricular noncompaction: a distinct cardiomyopathy or a trait shared by different cardiac diseases? J Am Coll Cardiol, 64: 1840-1850.
22. Gati S, Rajani R, Carr-White GS, Chambers JB. (2014) Adult left ventricular noncompaction: reappraisal of current diagnostic imaging modalities. JACC Cardiovasc Imaging, 7: 1266-1275.
23. Ichida F. (2020) Left ventricular noncompaction - Risk stratification and genetic consideration. J Cardiol, 75: 1-9.
24. Vergani V, Lazzeroni D, Peretto G. (2020) Bridging the gap between hypertrabeculation phenotype, noncompaction phenotype and left ventricular noncompaction cardiomyopathy. J Cardiovasc Med (Hagerstown), 21: 192-199.
25. Finsterer J, Stollberger C. (2020) Left Ventricular Noncompaction Syndrome: Genetic Insights and Therapeutic Perspectives. Curr Cardiol Rep, 22: 84.
26. Aung N, Doimo S, Ricci F, Sanghvi MM, Pedrosa C, Woodbridge SP, Al-Balah A, Zemrak F, Khanji MY, Munroe PB, Naci H, Petersen SE. (2020) Prognostic Significance of Left Ventricular Noncompaction: Systematic Review and Meta-Analysis of Observational Studies. Circ Cardiovasc Imaging, 13: e009712.
27. Arbustini E, Favalli V, Narula N, Serio A, Grasso M. (2016) Left Ventricular Noncompaction: A Distinct Genetic Cardiomyopathy? J Am Coll Cardiol, 68: 949-966.
28. Stahli BE, Gebhard C, Biaggi P, Klaassen S, Valsangiacomo Buechel E, Attenhofer Jost CH, Jenni R, Tanner FC, Greutmann M. (2013) Left ventricular non-compaction: prevalence in congenital heart disease. Int J Cardiol, 167: 2477-2481.
29. Piga A, Longo F, Musallam KM, Veltri A, Ferroni F, Chiribiri A, Bonamini R. (2012) Left ventricular noncompaction in patients with beta-thalassemia: uncovering a previously unrecognized abnormality. Am J Hematol, 87: 1079-1083.

30. Gati S, Papadakis M, Van Niekerk N, Reed M, Yeghen T, Sharma S. (2013) Increased left ventricular trabeculation in individuals with sickle cell anaemia: physiology or pathology? Int J Cardiol, 168: 1658-1660.
31. Markovic NS, Dimkovic N, Damjanovic T, Loncar G, Dimkovic S. (2008) Isolated ventricular noncompaction in patients with chronic renal failure. Clin Nephrol, 70: 72-76.
32. Forder JR, Pohost GM. (2003) Cardiovascular nuclear magnetic resonance: basic and clinical applications. J Clin Invest, 111: 1630-1639.
33. Schulz-Menger J, Bluemke DA, Bremerich J, Flamm SD, Fogel MA, Friedrich MG, Kim RJ, von Knobelsdorff-Brenkenhoff F, Kramer CM, Pennell DJ, Plein S, Nagel E. (2020) Standardized image interpretation and post-processing in cardiovascular magnetic resonance - 2020 update : Society for Cardiovascular Magnetic Resonance (SCMR): Board of Trustees Task Force on Standardized Post-Processing. J Cardiovasc Magn Reson, 22: 19.
34. Berlot B, Bucciarelli-Ducci C, Palazzuoli A, Marino P. (2020) Myocardial phenotypes and dysfunction in HFpEF and HFrEF assessed by echocardiography and cardiac magnetic resonance. Heart Fail Rev, 25: 75-84.
35. Arnold JR, McCann GP. (2020) Cardiovascular magnetic resonance: applications and practical considerations for the general cardiologist. Heart, 106: 174-181.
36. Karamitsos TD, Arvanitaki A, Karvounis H, Neubauer S, Ferreira VM. (2020) Myocardial Tissue Characterization and Fibrosis by Imaging. JACC Cardiovasc Imaging, 13: 1221-1234.
37. Takehara Y. (2020) 4D Flow when and how? Radiol Med, 125: 838-850.
38. Chin TK, Perloff JK, Williams RG, Jue K, Mohrmann R. (1990) Isolated noncompaction of left ventricular myocardium. A study of eight cases. Circulation, 82: 507-513.
39. Diwadkar S, Nallamshetty L, Rojas C, Athienitis A, Declue C, Cox C, Patel A, Chae SH. (2017) Echocardiography fails to detect left ventricular noncompaction in a cohort of patients with noncompaction on cardiac magnetic resonance imaging. Clin Cardiol, 40: 364-369.
40. Chebrolu LH, Mehta AM, Nanda NC. (2017) Noncompaction cardiomyopathy: The role of advanced multimodality imaging techniques in diagnosis and assessment. Echocardiography, 34: 279-289.

41. Jacquier A, Thuny F, Jop B, Giorgi R, Cohen F, Gaubert JY, Vidal V, Bartoli JM, Habib G, Moulin G. (2010) Measurement of trabeculated left ventricular mass using cardiac magnetic resonance imaging in the diagnosis of left ventricular non-compaction. Eur Heart J, 31: 1098-1104.
42. Grothoff M, Pachowsky M, Hoffmann J, Posch M, Klaassen S, Lehmkuhl L, Gutberlet M. (2012) Value of cardiovascular MR in diagnosing left ventricular non-compaction cardiomyopathy and in discriminating between other cardiomyopathies. Eur Radiol, 22: 2699-2709.
43. Captur G, Muthurangu V, Cook C, Flett AS, Wilson R, Barison A, Sado DM, Anderson S, McKenna WJ, Mohun TJ, Elliott PM, Moon JC. (2013) Quantification of left ventricular trabeculae using fractal analysis. J Cardiovasc Magn Reson, 15: 36.
44. Grigoratos C, Barison A, Ivanov A, Andreini D, Amzulescu MS, Mazurkiewicz L, De Luca A, Grzybowski J, Masci PG, Marczak M, Heitner JF, Schwitter J, Gerber BL, Emdin M, Aquaro GD. (2019) Meta-Analysis of the Prognostic Role of Late Gadolinium Enhancement and Global Systolic Impairment in Left Ventricular Noncompaction. JACC Cardiovasc Imaging, 12: 2141-2151.
45. Niemann M, Liu D, Hu K, Cikes M, Beer M, Herrmann S, Gaudron PD, Hillenbrand H, Voelker W, Ertl G, Weidemann F. (2012) Echocardiographic quantification of regional deformation helps to distinguish isolated left ventricular non-compaction from dilated cardiomyopathy. Eur J Heart Fail, 14: 155-161.
46. Huttin O, Venner C, Frikha Z, Voilliot D, Marie PY, Aliot E, Sadoul N, Juilliere Y, Brembilla-Perrot B, Selton-Suty C. (2014) Myocardial deformation pattern in left ventricular non-compaction: Comparison with dilated cardiomyopathy. Int J Cardiol Heart Vasc, 5: 9-14.
47. van Dalen BM, Caliskan K, Soliman OI, Kauer F, van der Zwaan HB, Vletter WB, van Vark LC, Ten Cate FJ, Geleijnse ML. (2011) Diagnostic value of rigid body rotation in noncompaction cardiomyopathy. J Am Soc Echocardiogr, 24: 548-555.
48. Papavassiliu T, Kühl HP, Schröder M, Süselbeck T, Bondarenko O, Böhm CK, Beek A, Hofman MM, van Rossum AC. (2005) Effect of endocardial trabeculae on left ventricular measurements and measurement reproducibility at cardiovascular MR imaging. Radiology, 236: 57-64.
49. Riffel JH, Schmucker K, Andre F, Ochs M, Hirschberg K, Schaub E, Fritz T, Mueller-Hennessen M, Giannitsis E, Katus HA, Friedrich MG. (2019) Cardiovascular magnetic

resonance of cardiac morphology and function: impact of different strategies of contour drawing and indexing. Clin Res Cardiol, 108: 411-429.

50. Csecs I, Czimbalmos C, Suhai FI, Mikle R, Mirzahosseini A, Dohy Z, Szucs A, Kiss AR, Simor T, Toth A, Merkely B, Vago H. (2018) Left and right ventricular parameters corrected with threshold-based quantification method in a normal cohort analyzed by three independent observers with various training-degree. Int J Cardiovasc Imaging, 34: 1127-1133.
51. Janik M, Cham MD, Ross MI, Wang Y, Codella N, Min JK, Prince MR, Manoushagian S, Okin PM, Devereux RB, Weinsaft JW. (2008) Effects of papillary muscles and trabeculae on left ventricular quantification: increased impact of methodological variability in patients with left ventricular hypertrophy. J Hypertens, 26: 1677-1685.
52. Hautvast GL, Salton CJ, Chuang ML, Breeuwer M, O'Donnell CJ, Manning WJ. (2012) Accurate computer-aided quantification of left ventricular parameters: experience in 1555 cardiac magnetic resonance studies from the Framingham Heart Study. Magn Reson Med, 67: 1478-1486.
53. Jaspers K, Freling HG, van Wijk K, Romijn EI, Greuter MJ, Willems TP. (2013) Improving the reproducibility of MR-derived left ventricular volume and function measurements with a semi-automatic threshold-based segmentation algorithm. Int J Cardiovasc Imaging, 29: 617-623.
54. Bricq S, Frandon J, Bernard M, Guye M, Finas M, Marcadet L, Miquerol L, Kober F, Habib G, Fagret D, Jacquier A, Lalande A. (2016) Semiautomatic detection of myocardial contours in order to investigate normal values of the left ventricular trabeculated mass using MRI. J Magn Reson Imaging, 43: 1398-1406.
55. Varga-Szemes A, Muscogiuri G, Schoepf UJ, Wichmann JL, Suranyi P, De Cecco CN, Cannao PM, Renker M, Mangold S, Fox MA, Ruzsics B. (2016) Clinical feasibility of a myocardial signal intensity threshold-based semi-automated cardiac magnetic resonance segmentation method. Eur Radiol, 26: 1503-1511.
56. Espe EKS, Bendiksen BA, Zhang L, Sjaastad I. (2021) Analysis of right ventricular mass from magnetic resonance imaging data: a simple post-processing algorithm for correction of partial-volume effects. Am J Physiol Heart Circ Physiol, 320: H912-H922.
57. Amzulescu MS, De Craene M, Langet H, Pasquet A, Vancraeynest D, Pouleur AC, Vanoverschelde JL, Gerber BL. (2019) Myocardial strain imaging: review of general principles, validation, and sources of discrepancies. Eur Heart J Cardiovasc Imaging, 20: 605-619.

58. Scatteia A, Baritussio A, Bucciarelli-Ducci C. (2017) Strain imaging using cardiac magnetic resonance. Heart Fail Rev, 22: 465-476.
59. Zerhouni EA, Parish DM, Rogers WJ, Yang A, Shapiro EP. (1988) Human heart: tagging with MR imaging--a method for noninvasive assessment of myocardial motion. Radiology, 169: 59-63.
60. Bucius P, Erley J, Tanacli R, Zieschang V, Giusca S, Korosoglou G, Steen H, Stehning C, Pieske B, Pieske-Kraigher E, Schuster A, Lapinskas T, Kelle S. (2020) Comparison of feature tracking, fast-SENC, and myocardial tagging for global and segmental left ventricular strain. ESC Heart Fail, 7: 523-532.
61. D'Silva A, Jensen B. (2021) Left ventricular non-compaction cardiomyopathy: how many needles in the haystack? Heart, 107: 1344-1352.
62. Oechslin E, Jenni R, Klaassen S. (2021) Left Ventricular Noncompaction Is a Myocardial Phenotype: Cardiomyopathy-Yes or No? Can J Cardiol, 37: 366-369.
63. Jacquier A, Thuny F, Jop B, Giorgi R, Cohen F, Gaubert J-Y, Vidal V, Bartoli JM, Habib G, Moulin G. (2010) Measurement of trabeculated left ventricular mass using cardiac magnetic resonance imaging in the diagnosis of left ventricular non-compaction†. European Heart Journal, 31: 1098-1104.
64. Kuetting DL, Dabir D, Homsi R, Sprinkart AM, Luetkens J, Schild HH, Thomas DK. (2016) The effects of extracellular contrast agent (Gadobutrol) on the precision and reproducibility of cardiovascular magnetic resonance feature tracking. J Cardiovasc Magn Reson, 18: 30.
65. Szűcs A, Kiss AR, Suhai FI, Tóth A, Gregor Z, Horváth M, Czimbalmos C, Csécs I, Dohy Z, Szabó LE, Merkely B, Vágó H. (2019) The effect of contrast agents on left ventricular parameters calculated by a threshold-based software module: does it truly matter? The international journal of cardiovascular imaging, 35: 1683-1689.
66. Szucs A, Kiss AR, Suhai FI, Toth A, Gregor Z, Horvath M, Czimbalmos C, Csecs I, Dohy Z, Szabo LE, Merkely B, Vago H. (2019) The effect of contrast agents on left ventricular parameters calculated by a threshold-based software module: does it truly matter? Int J Cardiovasc Imaging, doi:10.1007/s10554-019-01587-9.
67. Schuster A, Hor KN, Kowallick JT, Beerbaum P, Kutty S. (2016) Cardiovascular Magnetic Resonance Myocardial Feature Tracking: Concepts and Clinical Applications. Circ Cardiovasc Imaging, 9: e004077.
68. Mosteller RD. (1987) Simplified calculation of body-surface area. N Engl J Med, 317: 1098.

69. Alfakih K, Plein S, Thiele H, Jones T, Ridgway JP, Sivananthan MU. (2003) Normal human left and right ventricular dimensions for MRI as assessed by turbo gradient echo and steady-state free precession imaging sequences. J Magn Reson Imaging, 17: 323-329.
70. Cerqueira MD, Weissman NJ, Dilsizian V, Jacobs AK, Kaul S, Laskey WK, Pennell DJ, Rumberger JA, Ryan T, Verani MS, American Heart Association Writing Group on Myocardial S, Registration for Cardiac I. (2002) Standardized myocardial segmentation and nomenclature for tomographic imaging of the heart. A statement for healthcare professionals from the Cardiac Imaging Committee of the Council on Clinical Cardiology of the American Heart Association. Circulation, 105: 539-542.
71. Katz J, Milliken MC, Stray-Gundersen J, Buja LM, Parkey RW, Mitchell JH, Peshock RM. (1988) Estimation of human myocardial mass with MR imaging. Radiology, 169: 495-498.
72. Sechtem U, Pflugfelder PW, Gould RG, Cassidy MM, Higgins CB. (1987) Measurement of right and left ventricular volumes in healthy individuals with cine MR imaging. Radiology, 163: 697-702.
73. Grothues F, Moon JC, Bellenger NG, Smith GS, Klein HU, Pennell DJ. (2004) Interstudy reproducibility of right ventricular volumes, function, and mass with cardiovascular magnetic resonance. American Heart Journal, 147: 218-223.
74. Semelka RC, Tomei E, Wagner S, Mayo J, Kondo C, Suzuki J, Caputo GR, Higgins CB. (1990) Normal left ventricular dimensions and function: interstudy reproducibility of measurements with cine MR imaging. Radiology, 174: 763-768.
75. Jaspers K, Freling HG, van Wijk K, Romijn EI, Greuter MJW, Willems TPJTIJoCI. (2013) Improving the reproducibility of MR-derived left ventricular volume and function measurements with a semi-automatic threshold-based segmentation algorithm. 29: 617-623.
76. Krombach GA, Plum T, Koos R, Hoffmann R, Altiok E, Krämer NA, Günther RW, Schoth FJER. (2011) Functional cardiac MR imaging with true fast imaging with steady-state free precession before and after intravenous injection of contrast medium: comparison of image quality and accuracy. 21: 702-711.
77. Pennell DJ, Underwood SR, Longmore DB. (1993) Improved cine MR imaging of left ventricular wall motion with gadopentetate dimeglumine. Journal of Magnetic Resonance Imaging, 3: 13-19.

78. Kirsch JE. (1991) Basic principles of magnetic resonance contrast agents. Top Magn Reson Imaging, 3: 1-18.
79. Xiao YD, Paudel R, Liu J, Ma C, Zhang ZS, Zhou SK. (2016) MRI contrast agents: Classification and application (Review). Int J Mol Med, 38: 1319-1326.
80. Scott LJJCDI. (2013) Gadobutrol: A Review of Its Use for Contrast-Enhanced Magnetic Resonance Imaging in Adults and Children. 33: 303-314.
81. Seale MK, Catalano OA, Saini S, Hahn PF, Sahani DV. (2009) Hepatobiliary-specific MR Contrast Agents: Role in Imaging the Liver and Biliary Tree. 29: 1725-1748.
82. Wildgruber M, Stadlbauer T, Rasper M, Hapfelmeier A, Zelger O, Eckstein HH, Halle M, Rummeny EJ, Huber AM. (2014) Single-dose gadobutrol in comparison with single-dose gadobenate dimeglumine for magnetic resonance imaging of chronic myocardial infarction at 3 T. Invest Radiol, 49: 728-734.
83. Ivanov A, Dabiesingh DS, Bhumireddy GP, Mohamed A, Asfour A, Briggs WM, Ho J, Khan SA, Grossman A, Klem I, Sacchi TJ, Heitner JF. (2017) Prevalence and Prognostic Significance of Left Ventricular Noncompaction in Patients Referred for Cardiac Magnetic Resonance Imaging. Circ Cardiovasc Imaging, 10.
84. Negri F, De Luca A, Fabris E, Korcova R, Cernetti C, Grigoratos C, Aquaro GD, Nucifora G, Camici PG, Sinagra G. (2019) Left ventricular noncompaction, morphological, and clinical features for an integrated diagnosis. Heart Fail Rev, 24: 315-323.
85. Dreisbach JG, Mathur S, Houbois CP, Oechslin E, Ross H, Hanneman K, Wintersperger BJ. (2020) Cardiovascular magnetic resonance based diagnosis of left ventricular non-compaction cardiomyopathy: impact of cine bSSFP strain analysis. J Cardiovasc Magn Reson, 22: 9.
86. Stokke TM, Hasselberg NE, Smedsrud MK, Sarvari SI, Haugaa KH, Smiseth OA, Edvardsen T, Remme EW. (2017) Geometry as a Confounder When Assessing Ventricular Systolic Function: Comparison Between Ejection Fraction and Strain. J Am Coll Cardiol, 70: 942-954.
87. Andre F, Steen H, Matheis P, Westkott M, Breuninger K, Sander Y, Kammerer R, Galuschky C, Giannitsis E, Korosoglou G, Katus HA, Buss SJ. (2015) Age- and gender-related normal left ventricular deformation assessed by cardiovascular magnetic resonance feature tracking. J Cardiovasc Magn Reson, 17: 25.
88. Menting ME, McGhie JS, Koopman LP, Vletter WB, Helbing WA, van den Bosch AE, Roos-Hesselink JW. (2016) Normal myocardial strain values using 2D speckle tracking

echocardiography in healthy adults aged 20 to 72 years. Echocardiography, 33: 1665-1675.

89. Yubbu P, Nawaytou HM, Calderon-Anyosa R, Banerjee A. (2018) Diagnostic value of myocardial deformation pattern in children with noncompaction cardiomyopathy. Int J Cardiovasc Imaging, 34: 1529-1539.

90. Kawel-Boehm N, McClelland RL, Zemrak F, Captur G, Hundley WG, Liu CY, Moon JC, Petersen SE, Ambale-Venkatesh B, Lima JAC, Bluemke DA. (2017) Hypertrabeculated Left Ventricular Myocardium in Relationship to Myocardial Function and Fibrosis: The Multi-Ethnic Study of Atherosclerosis. Radiology, 284: 667-675.

91. Verdugo-Marchese M, Coiro S, Selton-Suty C, Kobayashi M, Bozec E, Lamiral Z, Venner C, Zannad F, Rossignol P, Girerd N, Huttin O. (2020) Left ventricular myocardial deformation pattern, mechanical dispersion, and their relation with electrocardiogram markers in the large population-based STANISLAS cohort: insights into electromechanical coupling. Eur Heart J Cardiovasc Imaging, doi:10.1093/ehjci/jeaa148.

92. Jalanko M, Tarkiainen M, Sipola P, Jaaskelainen P, Lauerma K, Laine M, Nieminen MS, Laakso M, Helio T, Kuusisto J. (2016) Left ventricular mechanical dispersion is associated with nonsustained ventricular tachycardia in hypertrophic cardiomyopathy. Ann Med, 48: 417-427.

93. Ermakov S, Gulhar R, Lim L, Bibby D, Fang Q, Nah G, Abraham TP, Schiller NB, Delling FN. (2019) Left ventricular mechanical dispersion predicts arrhythmic risk in mitral valve prolapse. Heart, 105: 1063-1069.

94. Astrom Aneq M, Maret E, Brudin L, Svensson A, Engvall J. (2018) Right ventricular systolic function and mechanical dispersion identify patients with arrhythmogenic right ventricular cardiomyopathy. Clin Physiol Funct Imaging, 38: 779-787.

95. Claus P, Omar AMS, Pedrizzetti G, Sengupta PP, Nagel E. (2015) Tissue Tracking Technology for Assessing Cardiac Mechanics: Principles, Normal Values, and Clinical Applications. JACC Cardiovasc Imaging, 8: 1444-1460.

96. Kutty S, Rangamani S, Venkataraman J, Li L, Schuster A, Fletcher SE, Danford DA, Beerbaum P. (2013) Reduced global longitudinal and radial strain with normal left ventricular ejection fraction late after effective repair of aortic coarctation: a CMR feature tracking study. Int J Cardiovasc Imaging, 29: 141-150.

97. Yousef ZR, Foley PW, Khadjooi K, Chalil S, Sandman H, Mohammed NU, Leyva F. (2009) Left ventricular non-compaction: clinical features and cardiovascular magnetic resonance imaging. BMC Cardiovasc Disord, 9: 37.
98. Arenas IA, Mihos CG, DeFaria Yeh D, Yucel E, Elmahdy HM, Santana O. (2018) Echocardiographic and clinical markers of left ventricular ejection fraction and moderate or greater systolic dysfunction in left ventricular noncompaction cardiomyopathy. Echocardiography, 35: 941-948.
99. Kiss AR, Gregor Z, Furak A, Toth A, Horvath M, Szabo L, Czimbalmos C, Dohy Z, Merkely B, Vago H, Szucs A. (2021) Left ventricular characteristics of noncompaction phenotype patients with good ejection fraction measured with cardiac magnetic resonance. Anatol J Cardiol, 25: 565-571.
100. Onishi T, Saha SK, Delgado-Montero A, Ludwig DR, Onishi T, Schelbert EB, Schwartzman D, Gorcsan J, 3rd. (2015) Global longitudinal strain and global circumferential strain by speckle-tracking echocardiography and feature-tracking cardiac magnetic resonance imaging: comparison with left ventricular ejection fraction. J Am Soc Echocardiogr, 28: 587-596.
101. Lima MSM, Villarraga HR, Abduch MCD, Lima MF, Cruz CBBV, Sbano JCN, Voos MC, Mathias WJ, Tsutsui JM. (2017) Global Longitudinal Strain or Left Ventricular Twist and Torsion? Which Correlates Best with Ejection Fraction? Arquivos brasileiros de cardiologia, 109: 23-29.
102. Arunamata A, Stringer J, Balasubramanian S, Tacy TA, Silverman NH, Punn R. (2019) Cardiac Segmental Strain Analysis in Pediatric Left Ventricular Noncompaction Cardiomyopathy. J Am Soc Echocardiogr, 32: 763-773 e761.
103. Muser D, Castro SA, Santangeli P, Nucifora G. (2018) Clinical applications of feature-tracking cardiac magnetic resonance imaging. World J Cardiol, 10: 210-221.
104. Gastl M, Gotschy A, Polacin M, Vishnevskiy V, Meyer D, Sokolska J, Tanner FC, Alkadhi H, Kozerke S, Manka R. (2019) Determinants of myocardial function characterized by CMR-derived strain parameters in left ventricular non-compaction cardiomyopathy. Sci Rep, 9: 15882.
105. Nucifora G, Sree Raman K, Muser D, Shah R, Perry R, Awang Ramli KA, Selvanayagam JB. (2017) Cardiac magnetic resonance evaluation of left ventricular functional, morphological, and structural features in children and adolescents vs. young adults with isolated left ventricular non-compaction. Int J Cardiol, 246: 68-73.

106. Pu C, Hu X, Ye Y, Lv S, Fei J, Albaqali S, Hu H. (2020) Evaluation of myocardial deformation pattern of left ventricular noncompaction by cardiac magnetic resonance tissue tracking. Kardiol Pol, 78: 71-74.
107. Cai J, Bryant JA, Le T-T, Su B, de Marvao A, O'Regan DP, Cook SA, Chin CW-L. (2017) Fractal analysis of left ventricular trabeculations is associated with impaired myocardial deformation in healthy Chinese. Journal of Cardiovascular Magnetic Resonance, 19: 102.
108. Bogaert J, Rademakers FE. (2001) Regional nonuniformity of normal adult human left ventricle. Am J Physiol Heart Circ Physiol, 280: H610-620.
109. Haland TF, Saberniak J, Leren IS, Edvardsen T, Haugaa KH. (2017) Echocardiographic comparison between left ventricular non-compaction and hypertrophic cardiomyopathy. International Journal of Cardiology, 228: 900-905.
110. Pan J, Wan Q, Li J, Wu H, Gao C, Tao Y, Wei M. (2018) Strain Values of Left Ventricular Segments Reduce Non-homogeneously in Dilated Cardiomyopathy with Moderately and Severely Deteriorated Heart Function Assessed by MRI Tissue Tracking Imaging. Int Heart J, 59: 1312-1319.
111. Duan F, Xie M, Wang X, Li Y, He L, Jiang L, Fu Q. (2012) Preliminary clinical study of left ventricular myocardial strain in patients with non-ischemic dilated cardiomyopathy by three-dimensional speckle tracking imaging. Cardiovasc Ultrasound, 10: 8.
112. Aras D, Tufekcioglu O, Ergun K, Ozeke O, Yildiz A, Topaloglu S, Deveci B, Sahin O, Kisacik HL, Korkmaz S. (2006) Clinical features of isolated ventricular noncompaction in adults long-term clinical course, echocardiographic properties, and predictors of left ventricular failure. J Card Fail, 12: 726-733.
113. Feisst A, Kuetting DLR, Dabir D, Luetkens J, Homsi R, Schild HH, Thomas D. (2018) Influence of observer experience on cardiac magnetic resonance strain measurements using feature tracking and conventional tagging. Int J Cardiol Heart Vasc, 18: 46-51.
114. El Ghannudi S, Germain P, Jeung MY, Breton E, Croisille P, Durand E, Roy C, Gangi A. (2014) Quantification of left ventricular dyssynchrony in patients with systolic dysfunction: a comparison of circumferential strain MR-tagging metrics. J Magn Reson Imaging, 40: 1238-1246.
115. Yu CM, Lin H, Zhang Q, Sanderson JE. (2003) High prevalence of left ventricular systolic and diastolic asynchrony in patients with congestive heart failure and normal QRS duration. Heart, 89: 54-60.

116. Popescu BA, Beladan CC, Calin A, Muraru D, Deleanu D, Rosca M, Ginghina C. (2009) Left ventricular remodelling and torsional dynamics in dilated cardiomyopathy: reversed apical rotation as a marker of disease severity. Eur J Heart Fail, 11: 945-951.
117. Kim HK, Sohn DW, Lee SE, Choi SY, Park JS, Kim YJ, Oh BH, Park YB, Choi YS. (2007) Assessment of left ventricular rotation and torsion with two-dimensional speckle tracking echocardiography. J Am Soc Echocardiogr, 20: 45-53.
118. Maharaj N, Khandheria BK, Peters F, Libhaber E, Essop MR. (2013) Time to twist: marker of systolic dysfunction in Africans with hypertension. Eur Heart J Cardiovasc Imaging, 14: 358-365.
119. Nemes A, Foldeak D, Domsik P, Kalapos A, Sepp R, Borbenyi Z, Forster T. (2015) Different patterns of left ventricular rotational mechanics in cardiac amyloidosis-results from the three-dimensional speckle-tracking echocardiographic MAGYAR-Path Study. Quant Imaging Med Surg, 5: 853-857.
120. Nemes A, Havasi K, Domsik P, Kalapos A, Forster T. (2015) Can univentricular heart be associated with "rigid body rotation"? A case from the threedimensional speckle-tracking echocardiographic MAGYAR-path study. Hellenic J Cardiol, 56: 186-188.
121. Jin SM, Noh CI, Bae EJ, Choi JY, Yun YS. (2007) Decreased left ventricular torsion and untwisting in children with dilated cardiomyopathy. J Korean Med Sci, 22: 633-640.
122. Peters F, Khandheria BK, Libhaber E, Maharaj N, Dos Santos C, Matioda H, Essop MR. (2014) Left ventricular twist in left ventricular noncompaction. Eur Heart J Cardiovasc Imaging, 15: 48-55.
123. Notomi Y, Srinath G, Shiota T, Martin-Miklovic MG, Beachler L, Howell K, Oryszak SJ, Deserranno DG, Freed AD, Greenberg NL, Younoszai A, Thomas JD. (2006) Maturational and adaptive modulation of left ventricular torsional biomechanics: Doppler tissue imaging observation from infancy to adulthood. Circulation, 113: 2534-2541.

9. Bibliography of the Candidate's Publications

Publications related to dissertation

1. A Szucs*, **AR Kiss***, FI Suhai, A Toth, Zs Gregor, M Horvath, Cs Czimbalmos, I Csecs, Zs Dohy, LE Szabo, B Merkely, H Vago - The effect of contrast agents on left ventricular parameters calculated by a threshold-based software module – does it truly matter? International Journal of Cardiovascular Imaging. 2019;35(9):1683–1689. doi:10.1007/s10554-019-01587-9

   IF: 1.969

   *****A Szucs and AR Kiss contributed equally in this work.

2. A Szucs*, **AR Kiss***, Zs Gregor, M Horvath, A Toth, Zs Dohy, FI Suhai, B Merkely, H Vago – Changes in strain parameters at different deterioration levels of left ventricular function: a cardiac magnetic resonance feature-tracking study on noncompaction cardiomyopathy patients. International Journal of Cardiology 331 pp. 124-130. , 7 p. (2021). doi:10.1016/j.ijcard.2021.01.072

   IF: 4.164

   *****A Szucs and AR Kiss contributed equally in this work.

3. **AR Kiss**, A Szucs, A Toth, A Furak, Zs Gregor, M Horvath, LE Szabo, Cs Czimbalmos, B Merkely, H Vago - Left ventricular characteristics of noncompaction phenotype patients with good ejection fraction measured with cardiac magnetic resonance. The Anatolian Journal of Cardiology 25: 8 pp. 565-571., 7 p. (2021). doi:10.5152/AnatolJCardiol.2021.25905

   IF: 1.596

Publications not related to dissertation

1. I Csecs, Cs Czimbalmos, FI Suhai, R Mikle, A Mirzahosseini, Zs Dohy, A Szucs, **AR Kiss**, T Simor, A Toth, B Merkely, H Vago - Left and right ventricular parameters corrected with trabecular mass and papillary muscle in a normal cohort analyzed by three independent observers with various training-degree. International Journal of Cardiovascular Imaging. 2018;34(7):1127–1133. doi:10.1007/s10554-018-1322-4

   IF: 1.860

2. A Fabian, BK Lakatos, M Tokodi, **AR Kiss**, N Sydo, E Csulak, E Kispal, M Babity, A Szucs, O Kiss, B Merkely, A Kovacs – Geometrical remodeling of the mitral and tricuspid annuli in response to exercise training: 2 and 3D echocardiographic study in

elite athletes. American Journal of Physiology: Heart and Circulatory Physiology 320 : 5 pp. H1774-H1785. (2021). doi:10.1152/ajpheart.00877.2020

IF: 4.733

3. Zs Gregor, **AR Kiss**, LE Szabo, A Toth, K Grebur, M Horvath, Zs Dohy, B MErkely, H Vago, A Szucs – Sex- and age- specific normal values of left ventricular functional and myocardial mass parameters using threshold-based trabeculae quantification. PLOS ONE 16 10 p. e0258362 (2021)

   IF: 3.240

4. BK Lakatos, M Tokodi, A Fabian, Zs Ladanyi, H Vago, LE Szabo, N Sydo, E Csulak, O Kiss, M Babity, **AR Kiss**, Zs Gregor, A Szucs, B Merkely, A Kovacs - Frequent Constriction-Like Echocardiographic Findings in Elite Athletes Following Mild COVID-19: A Propensity Score-Matched Analysis. Frontiers in Cardiovascular Medicine (2297-055X): 8 Paper 760651. 8 p. (2022). doi: 10.3389/fcvm.2021.760651

   IF: 6.050

5. **AR Kiss**, Zs Gregor, A Furak, LE Szabo, Zs Dohy, B Merkely, H Vago, A Szucs - Age- and Sex-Specific Characteristics of Right Ventricular Compacted and Non-compacted Myocardium by Cardiac Magnetic Resonance. Frontiers in Cardiovascular Medicine (2297-055X): 8 Paper 781393. 10 p. (2021) doi:10.3389/fcvm.2021.781393

   IF: 6.050

6. A Fabian, A Ujvari, M Tokodi, BK Lakatos, O Kiss, M Babity, M Zamodics, N Sydo, E Csulak, H Vago, L Szabo, **AR Kiss**, A Szucs, B Merkely, A Kovacs - Biventricular mechanical pattern of the athlete’s heart: comprehensive characterization using 3D echocardiography. European Journal of Preventive Cardiology Paper: zwac026 (2022). doi: 10.1093/eurjpc/zwac026

   IF: 7,804

7. **AR Kiss**, Zs Gregor, A Popovics, K Grebur, LE Szabó, Zs Dohy, A Kovács, BK Lakatos, B Merkely, H Vágó, A Szűcs - Impact of Right Ventricular Trabeculation on Right Ventricular Function in Patients With Left Ventricular Non-compaction Phenotype. Frontiers In Cardiovascular Medicine 9 Paper: 843952 (2022). doi: 10.3389/fcvm.2022.843952

   IF: 6,050

10. Acknowledgments

I would like to thank my tutor **Professor Dr. Merkely Béla**, the rector of Semmelweis University, for giving me the opportunity to perform my PhD studies at the Semmelweis University Heart and Vascular Center and abroad. Thank you for always having time for me.

I would like to thank my greatest tutor **Dr. Andrea Szűcs** for her endless patience, care, knowledge, and support. Thank you for teaching me not only about research and cardiology but also about life in general. Thank you for the many opportunities that you have offered me.

I would like to thank **Dr. Zsófia Gregor**, who was my partner in crime in the past four years. My PhD years would have been less fruitful and enjoyable without your friendship, help and support.

I would like to thank **Dr. Hajnalka Vágó** for helping me with my research work. Thank you for your valuable comments on my manuscripts that always made them better.

I would like to thank **Dr. Attila Tóth**, who taught me the basics of CMR and medical statistics. Thank you for always helping me with this topic and for answering any kind of professional question.

I would like to thank **Dr. Márton Horváth, Dr. Liliána Szabó, Dr. Csilla Czimbalmos, Dr. Kinga Grebur, Dr. Zsófia Dohy,** and the student scientific researchers and for their help and support.